



Published in final edited form as:

*Curr Biol.* 2023 June 19; 33(12): 2367–2382.e7. doi:10.1016/j.cub.2023.04.050.

## Human scent guides mosquito thermotaxis and host selection under naturalistic conditions

Diego Giraldo<sup>1,6</sup>, Stephanie Rankin-Turner<sup>1,6</sup>, Abel Corver<sup>2,3</sup>, Genevieve M. Tauxe<sup>1</sup>, Anne L. Gao<sup>1</sup>, Dorian M. Jackson<sup>1</sup>, Limonty Simubali<sup>4</sup>, Christopher Book<sup>1,4</sup>, Jennifer C. Stevenson<sup>1,4</sup>, Philip E. Thuma<sup>1,4</sup>, Rajiv C. McCoy<sup>5</sup>, Andrew Gordus<sup>2,5</sup>, Monicah M. Mburu<sup>4</sup>, Edgar Simulundu<sup>4</sup>, Conor J. McMeniman<sup>1,2,7,\*</sup>

<sup>1</sup>W. Harry Feinstone Department of Molecular Microbiology and Immunology, Johns Hopkins Malaria Research Institute, Johns Hopkins Bloomberg School of Public Health, Johns Hopkins University, Baltimore, MD 21205, USA

<sup>2</sup>The Solomon H. Snyder Department of Neuroscience, Johns Hopkins University School of Medicine, Baltimore, MD 21205, USA

<sup>3</sup>Kavli Neuroscience Discovery Institute, Johns Hopkins University, Baltimore, MD 21218, USA

<sup>4</sup>Macha Research Trust, Choma District, PO Box 630166, Zambia

<sup>5</sup>Department of Biology, Johns Hopkins University, Baltimore, MD 21218, USA

<sup>6</sup>These authors contributed equally

<sup>7</sup>Lead contact

### SUMMARY

The African malaria mosquito *Anopheles gambiae* exhibits a strong innate drive to seek out humans in its sensory environment, classically entering homes to land on human skin in the hours flanking midnight. To gain insight into the role that olfactory cues emanating from the human body play in generating this epidemiologically important behavior, we developed a large-scale multi-choice preference assay in Zambia with infrared motion vision under semi-field conditions. We determined that *An. gambiae* prefers to land on arrayed visual targets warmed to human skin temperature during the nighttime when they are baited with carbon dioxide (CO<sub>2</sub>) emissions reflective of a large human over background air, body odor from one human over CO<sub>2</sub>, and the scent of one sleeping human over another. Applying integrative whole body volatilomics to multiple humans tested simultaneously in competition in a six-choice assay, we reveal high

\*Correspondence: cmcmeni1@jhu.edu.

#### AUTHOR CONTRIBUTIONS

Conceptualization, D.G., S.R.-T., J.C.S., and C.J.M.; data curation, D.G., S.R.-T., and A.C.; formal analysis, D.G., S.R.-T., A.C., A.L.G., D.M.J., R.C.M., and A.G.; funding acquisition: C.J.M.; investigation: D.G., S.R.-T., A.L.G., and D.M.J.; methodology: D.G., S.R.-T., A.C., G.M.T., A.L.G., D.M.J., C.B., A.G., and C.J.M.; project administration: L.S., C.B., J.C.S., P.E.T., M.M.M., E.S., and C.J.M.; visualization: D.G., S.R.-T., A.C., R.C.M., A.G., and C.J.M.; writing – original draft, D.G., S.R.-T., A.C., R.C.M., A.G., and C.J.M.; writing – review & editing, all authors.

#### SUPPLEMENTAL INFORMATION

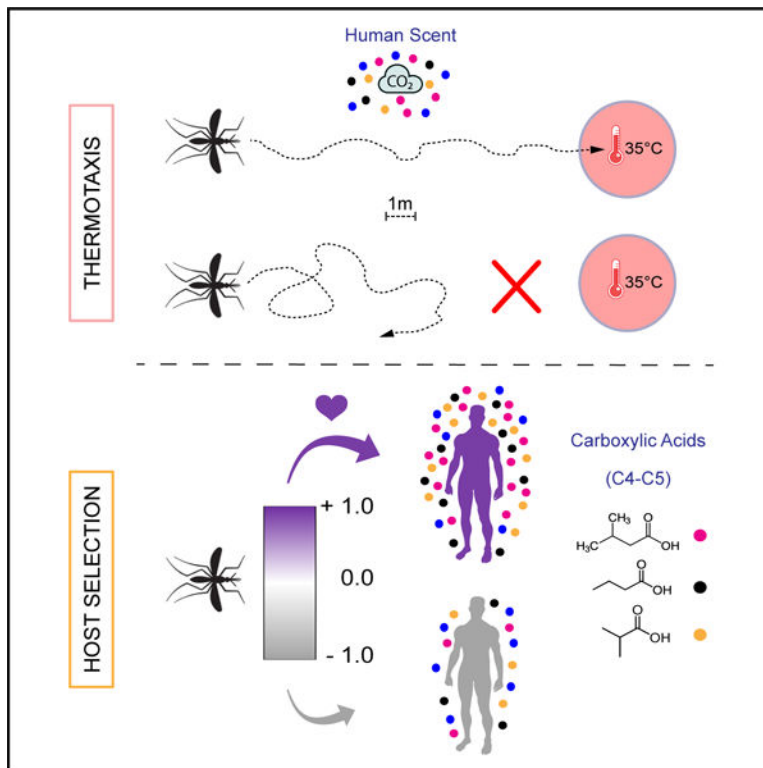
Supplemental information can be found online at <https://doi.org/10.1016/j.cub.2023.04.050>.

#### DECLARATION OF INTERESTS

The authors declare no competing interests.

attractiveness is associated with whole body odor profiles from humans with increased relative abundances of the volatile carboxylic acids butyric acid, isobutyric acid, and isovaleric acid, and the skin microbe-generated methyl ketone acetoin. Conversely, those least preferred had whole body odor that was depleted of carboxylic acids among other compounds and enriched with the monoterpene eucalyptol. Across expansive spatial scales, heated targets without CO<sub>2</sub> or whole body odor were minimally or not attractive at all to *An. gambiae*. These results indicate that human scent acts critically to guide thermotaxis and host selection by this prolific malaria vector as it navigates towards humans, yielding intrinsic heterogeneity in human biting risk.

## Graphical abstract



## In brief

Giraldo et al. develop an expansive semi-field system for multi-choice assays of mosquito olfactory preference. They find human scent draws malaria mosquitoes to warmed targets mimicking human skin to guide mosquito thermotaxis behavior and host selection, with levels of certain air-borne carboxylic acids associated with attractiveness.

## INTRODUCTION

The African malaria mosquito *Anopheles gambiae* is a prolific vector of malaria throughout sub-Saharan Africa. This anthropophilic disease vector classically exhibits peak periods of host-seeking activity during the late evening and early mornings in the hours flanking midnight, when humans are typically sleeping.<sup>1</sup> During this time frame, humans are usually

indoors and housed in groups, where human whole body odor inclusive of carbon dioxide (CO<sub>2</sub>) and other volatile organic compounds found in skin odor and breath,<sup>2</sup> dissipates from each individual into the air. Human body odor from different humans rises on warm convective currents emanating from the skin to generate odor plumes that typically dissipate through the housing eaves<sup>3</sup> or walls to be carried downwind, providing an alluring olfactory stimulus for mosquitoes in the vicinity that indicates human presence.<sup>4,5</sup>

In addition to heat, CO<sub>2</sub>, and other constituent components of body odor, humans also emit moisture in exhaled breath and sweat and provide a conspicuous source of both static and moving visual contrast against their environmental surroundings. It has been demonstrated previously—primarily using varied laboratory behavioral paradigms,<sup>6–14</sup>—that all of these human-related sensory cues can be integrated synergistically to drive attractive behavioral responses in *An. gambiae* and related mosquito species. However, a vast majority of these studies have occurred within confined spatial scales of <0.5 m<sup>3</sup> in the laboratory; thus most likely illuminating the importance of such interactions within the context of close-range host-seeking behavior.

Due to their varying physical and chemical properties, human-related cues likely dissipate varied distances from the human body into the surrounding environment, with each cue uniquely guiding mosquito host-seeking behavior in combination with others as they navigate toward and land upon a target human host. For instance, although warmth from skin likely only dissipates approximately ~30–50 cm from the human body,<sup>8</sup> visual cues are likely detectable at a range of ~5–15 m,<sup>15</sup> whereas volatile body odorants such as CO<sub>2</sub> are hypothesized to be carried downwind and detected by hematophagous arthropods at a range of up to ~60 m.<sup>16</sup> During their hunt for humans, *An. gambiae* thus encounters a dynamic and complex sensory environment against the noisy backdrop of human habitation.

Furthermore, several studies have shown that there can be substantial variability in mosquito biting frequency toward humans in disease-endemic regions<sup>17</sup> and that some people are more attractive to malaria vectors relative to others.<sup>18–23</sup> Heterogeneity in mosquito biting preferences can lead to variation in infection risk and intensify the basic reproductive number of malaria, which can have important consequences in malaria epidemiology and control.<sup>17,24</sup> Different factors have been associated with variability in human attractiveness to mosquitoes such as pregnancy,<sup>23,25,26</sup> skin microbiota,<sup>27–29</sup> diet,<sup>30</sup> alcohol consumption,<sup>31,32</sup> stage-specific malaria parasite infection,<sup>33–35</sup> and human genetics.<sup>36,37</sup> Although these factors are all believed to influence the chemical composition of human body odor,<sup>29,34</sup> the specific components of human scent modulating differential attraction of *An. gambiae* to humans in naturalistic environments remain largely unexplored.

To gain insight into how olfactory cues emanating from the human body guide mosquito host-seeking behavior and modulate human attractiveness to *An. gambiae*, we have developed a large-scale, semi-field system in Zambia for multi-choice assays of mosquito olfactory preference. Using infrared video tracking in the hours surrounding midnight, we demonstrate that *An. gambiae* prefers to land on black, warmed targets mimicking human skin when they are baited with CO<sub>2</sub> emissions reflective of a large human over background air, body odor from one human over CO<sub>2</sub>, and the scent of one individual

over another. Using a six-choice assay configuration, we further use this system to screen for individuals whose scent is differentially attractive to *An. gambiae* and apply whole body volatilomics to identify human odorants with the potential to modulate attractiveness to this major disease vector. Our data indicate that at enhanced spatial scales, heat and visual cues alone are insufficient to trigger *An. gambiae* landing behavior, and CO<sub>2</sub> and whole body odor are required for long-range host-seeking behavior in this malaria vector. We reveal high attractiveness is associated with whole body odor profiles from sleeping humans with increased relative abundances of the volatile carboxylic acids butyric acid, isobutyric acid, and isovaleric acid as well as the skin microbe-generated methyl ketone acetoin, among others. Conversely, those least preferred had whole body odor that was depleted of carboxylic acids among other compounds and enriched with the monoterpene eucalyptol. We propose that across expansive spatial scales human scent guides mosquito thermotaxis and host selection, yielding heterogeneity in human biting risk underlying malaria transmission.

## RESULTS

### Development of the odor-guided thermotaxis assay to quantify *An. gambiae* landing behavior under low-light conditions at night

To generate an optimized assay configuration to mimic the process of landing on human skin, with the potential to be scaled for use in mosquito multi-choice host preference assays, we first engineered a novel behavioral apparatus customized for scoring *An. gambiae* landing behavior in the presence of heat and olfactory stimuli under low-light conditions at night (~0.04 lux, mimicking nighttime moonlighting<sup>38</sup>). The odor-guided thermotaxis assay (OGTA) uses infrared videography to quantify landings of female *An. gambiae* on a black aluminum disc (10 cm in diameter) heated to mimic human skin temperature (35°C) that can be baited with any target olfactory stimulus using controlled airflow (Figure 1A). The heated landing platform was illuminated with an infrared array which allowed us to focus on mosquitoes that landed on the platform (Figure 1B) and obtain their 2D trajectories. Mosquitoes hovering or flying over the platform were not illuminated and would not be detected by the camera or would appear as fast-moving blurs that were not included in the analysis. We designed all OGTA components to be powered using 12-volt batteries to facilitate high-content recordings of mosquito landing behavior in “off-the-grid” settings typically encountered under semi-field and field environments situated at remote localities in Africa.

To validate the utility of the OGTA to score odor-guided thermotaxis from *An. gambiae*, we first performed behavioral trials examining multimodal synergisms between the host-related cues CO<sub>2</sub> and heat at close range in the laboratory, while simulating nighttime light conditions. During these assays a single OGTA platform was centrally positioned at the base of a small cage (30 cm × 30 cm × 30 cm) with a volume of 0.027 m<sup>3</sup>. Strikingly, when CO<sub>2</sub> and heat were co-presented as stimuli in these assays, high levels of landings were observed (Figures 1C–1E). In particular, each pulse of CO<sub>2</sub> triggered significant levels of landings on the heated platform that returned to baseline levels within 15 min (Figure 1D). In contrast, trials with a synthetic air stimulus with heat triggered very few landings.

Similarly, CO<sub>2</sub> pulses without heat yielded a similarly low number of landings. Control assays with synthetic air without heat, or no stimuli at all, elicited even lower levels of landings.

We conclude that the OGTA is a powerful method to quantify *An. gambiae* landing behavior under low-light conditions at night, and that CO<sub>2</sub> and heat potentially synergize together to evoke landing behavior at close range in this primary malaria vector.

### **A semi-field system for multi-choice assays of mosquito olfactory preference**

To develop an expansive arena for multi-choice assays of *An. gambiae* olfactory preference with arrays of OGTA in competition, we next engineered and constructed a large-scale, semi-field system at Macha, Choma District, Zambia (Figure 2). This system consists of a central screened flight cage (20 m × 20 m × 2.5 m) with a volume of 1,000 m<sup>3</sup> for contained assays of *An. gambiae* olfactory preference that is flanked at its perimeter by up to eight one-person tents (Figures 2A and 2B). Each tent is connected to the central cage by screened aluminum ducting with a low-speed fan to directionally pipe target olfactory cues placed inside them, including whole body odor from sleeping humans or CO<sub>2</sub>, into the flight cage arena and directly onto concordant OGTA (Figures 2C and S1A) for exposure-free assays of mosquito olfactory preference. For use in the semi-field system, we modified the OGTA design to place the infrared-illuminated landing platform heated to 35°C and IR-sensitive camera on top of a standardized black container, with the screened ducting from each tent venting odor directly over this target (Figures 2D and S1B).

This semi-field system provides flexibility to perform anywhere from one-choice to eight-choice trials, by simply modifying the number of tents and OGTA used in experiments. In contrast to typical two-choice laboratory wind tunnels with volumes of ~0.5 m<sup>3</sup> (example dimensions: 2 m × 0.5 m × 0.5 m), our semi-field system provides a flight cage arena that is ~2,000-fold larger to assess *An. gambiae* olfactory preferences under more naturalistic conditions. Conveniently, separate insectaries located adjacent to the semi-field system facilitated use of the laboratory-reared Kisumu strain of *An. gambiae* of known age and physiological status for behavioral experimentation. A weather station (Figure 2A) was also installed adjacent to the flight cage to measure environmental parameters including wind speed and directionality, temperature, and humidity; and retrospectively monitor their effects on *An. gambiae* host-seeking behavior.

### ***An. gambiae* prefers heated targets baited with CO<sub>2</sub> emissions reflective of a large human relative to background air**

To initially validate the utility of this semi-field system to quantify mosquito olfactory preferences, we first tested choices of female *An. gambiae* to land on one heated OGTA platform baited with a CO<sub>2</sub> stimulus relative to seven heated platforms that were baited with only background air (Figures 3 and S1). We supplied a CO<sub>2</sub> stimulus that was 400 ppm above background atmospheric concentrations at the output of the ducting on the OGTA platform to reflect CO<sub>2</sub> emissions from a large human with a body weight of ~100 kg resting in a tent. For these trials, the eight OGTA were arrayed in an octagonal configuration in the center of the flight cage arena, with 6 replicate nightly assays occurring from 22:00–

4:00 hours (Figures 3A and S1C) during peak periods of *An. gambiae* circadian activity. Consistent with our previous laboratory assays (Figure 1), we observed a strong synergy between CO<sub>2</sub> and heat under semi-field conditions, with these cues eliciting high levels of landings only on the platform where these stimuli were co-presented (Figures 3B and 3C). In contrast, very few landings were observed on the other seven heated platforms baited only with background air.

As the total number of landings varied every night (Figure S1D), we subsequently calculated the relative attractiveness of each platform over replicate nightly trials (Figure 3D). To confirm that differences in landings we observed were indeed due to attractiveness of the stimuli presented and not the position that they occupied relative to the cage, we next carried out a permutation analysis. This consisted of simulating the likelihood of observing the same landing percentage differences between each pair of platforms, under the null hypothesis that such biases arise only from position preference. This analysis indicated that the landing percentage differences observed between CO<sub>2</sub> baited and un-baited control platforms was highly unlikely due to position bias. Overall, a strong and significant preference was observed for the heated platform baited with CO<sub>2</sub> relative to the seven other heated platforms receiving only background air (Figure 3D).

Noticeably in this series of trials, wind appeared non-directional and wind speeds were very low (<0.2 m/s) (Figure S1E), and we did not observe any cross-contamination whereby CO<sub>2</sub> appeared to obviously yield landings on adjacent platforms baited with background environmental air. We conclude that CO<sub>2</sub> triggers landing behavior of *An. gambiae* on a heated artificial target mimicking human skin in a semi-field context, and heat alone is insufficient to evoke landings in this context at long range.

### ***An. gambiae* prefers heated targets baited with whole body odor of one human relative to CO<sub>2</sub>**

Volatile organic compounds (VOCs) present in human body odor have been found to synergize with CO<sub>2</sub> to enhance attraction during mosquito host-seeking behavior.<sup>6,39–41</sup> Human whole body odor itself is a complex blend of hundreds of VOCs found in skin odor and breath, inclusive of ~4% CO<sub>2</sub> exhaled in human breath. To test olfactory preferences of female *An. gambiae* for human whole body odor relative to CO<sub>2</sub> alone, we performed another eight-choice competition assay, whereby one heated OGTA platform was baited with whole body odor from one sleeping human subject weighing 76 kg, and a CO<sub>2</sub> stimulus of 400 ppm above background atmospheric concentrations (reflective of CO<sub>2</sub> emissions from a ~100kg human) was used to bait each of the seven other heated platforms (Figures 4A and S2A).

This multi-choice test revealed that *An. gambiae* strongly preferred to land on the heated OGTA platform baited with human whole body odor relative to the other heated platforms that were baited with CO<sub>2</sub> (Figures 4B–4D and S2B). Across 6 replicate nights of these assays, the human whole body odor-baited heated platform was significantly preferred over the CO<sub>2</sub>-baited heated platforms (Figures 4D and S2B). Interestingly, nights with lowest preference towards human odor were also nights with overall lower numbers of total landings (Figure S2B), indicative of low mosquito activity.



In human odor-baited platforms, we observed a second peak of activity around midnight (Figure 4C), indicating that mosquitoes may be revisiting this specific platform during the night since it is the only source of a highly attractive stimulus. Similar to the previous trials, we determined that wind speed across replicate nights in the semi-field system during this series of trials was extremely low (Figure S2C) and we found no clear indication of cross-contamination, whereby any of the CO<sub>2</sub> platforms immediately adjacent to the platform baited with human whole body odor had high levels of landing. These results demonstrate that *An. gambiae* strongly prefers 35°C targets baited with whole body odor of one human relative to CO<sub>2</sub> alone.

### ***An. gambiae* prefers heated targets baited with the scent of one human over another**

We next used the semi-field system in an eight-choice format to test whether female *An. gambiae* would exhibit olfactory preferences between two humans (Figures 5 and S3). In these assays performed over seven replicate nights, two heated OGTA platforms were baited with whole body odor from two human subjects sleeping in separate tents, while the six other heated platforms were baited only with background air (Figures 5A and S3A). During these assays, we observed that heated platforms that were only baited with background air received no landings (Figures 5B–5D and S3B). In contrast, high levels of landings were observed on both of the heated platforms baited with whole body odor from either human.

For both human subjects, we observed an initial peak in landing activity on the heated platforms within the first hour, followed by a sustained period of constant landing that was maintained throughout the assay period (Figure 5C). Noticeably, six out of seven nights the heated platform that was baited with whole body odor from Human 2 (weighing 73 kg) received approximately double the number of landings relative to the heated platform baited with whole body odor from Human 1 (weighing 76 kg, the same individual tested in the one-human experiment above). A permutation analysis revealed that these differences were significant regardless of the position in the cage that the human subjects occupied (Figures 5D and S3B). When considered in pairwise competition, a significant preference index for Human 2 over Human 1 was observed (Figure 5E). Furthermore, this preference index was not influenced by the distance between the heated platforms baited with whole body odor from each of these human subjects (Figure 5F); for instance, whether or not they were immediately adjacent to one another or farther away from each other. Interestingly, the total landings measured when odor of two humans was introduced into the flight cage was higher than when scent of a single human was introduced (Figures S2B and S3B). We believe this is due to an increased chance of a mosquito encountering an attractive cue in the large volume of the arena when whole body odor from two humans is present, which in turn can increase the host-seeking behavior of the mosquitoes in the cage.

In these trials, mean wind speeds were low (Figure S3C) and we saw no indication of cross-contamination between platforms, whereby high levels of landings were recorded on heated platforms baited with background air which were immediately adjacent to a heated platform with human whole body odor. As rotating human positions in this eight-choice assay configuration every night had no effect on the tendency of *An. gambiae* to choose body odorants derived from Human 2 relative to those from Human 1, we conclude that this

olfactory preference is likely due to differential attractiveness between whole body odor of these two humans, rather than position effects in the cage.

### ***An. gambiae* is differentially attracted to heated targets baited with the scent of certain individuals in a cohort of six humans**

To extend use of this multi-choice assay for *An. gambiae* olfactory preference to screen for differences in human attractiveness from larger groups of humans, we next tested a new cohort of six human subjects simultaneously in the semi-field system (Figures 6 and S4). This cohort included Human 1 from the one- and two-human experiments above, and five new humans (Humans 2–6). In this assay configuration over six replicate nights, six OGTA were arrayed in a hexagonal configuration within the flight cage (Figures 6A, S4A, and S4B), yielding 15 pairwise comparisons between the individuals in this cohort per night. Relative to two-choice assay formats, use of this configuration therefore increases the throughput of screening to rank individuals by attractiveness by 15-fold.

Since our previous experiments with two human subjects demonstrated that an olfactory preference is clearly observed during the first 3 h of experimentation (Figure 5C), we recorded mosquito landing activity during both an acclimation period from 21:30–22:00 hours during which time heated platforms were only baited with background air from empty subject tents, and then from 22:00–1:00 hours during which time the six humans occupied them. Consistent with the anthropophilic nature of *An. gambiae*, all six heated platforms baited with whole body odor from the human subjects yielded landings (Figures 6B, 6C, and S4C). Importantly, no activity was observed during the initial 30-min acclimation period, during which time the heated platforms were baited only with background air from the empty tents (Figure 6C), with landings starting as soon as whole body odor from each of the human was provided as an olfactory stimulus by humans entering the tents.

Across replicate nighttime trials, scent from Human 3 was observed to consistently be most attractive in this six-person cohort, on average having the highest number of landings and proportionally attracting the most mosquitoes on four out of the six nights tested (Figures 6C, 6D, and S4C). In contrast, scent from Human 2 elicited very low landing activity and proportionally had the lowest attractiveness on four of the six nights, while the remaining subjects had similar intermediate levels of attraction. When ranked in terms of mean attractiveness, Human 3 was the most attractive, followed by Humans 5, 1, 6, 4, with Human 2 being the least attractive (Figure 6D).

To evaluate the effects of humidity, temperature, position, and human subject on *An. gambiae* olfactory preference in this six-choice format, we next employed a generalized linear model framework. Specifically, we found that a negative binomial regression model provided good fit for the observed proportions of mosquito landings throughout replicate trials (Figure S5A). This analysis revealed that upon controlling for other variables, there was no significant effect of humidity or temperature on the preferences observed (Table S1). However, human subject identity was significantly associated with proportional landings (Likelihood-ratio test:  $\chi^2[5] = 19.62$ ;  $P = 1.47 \times 10^{-3}$ ). Post-hoc comparisons of pairwise marginal means revealed that Human 3 had the highest proportion of mosquito landings, differing significantly from Humans 2 and 4, while Human 2 had the lowest



proportion of landings, differing from Humans 1, 3 and 5 (Figure S5B). Moreover, under the same modeling framework, we found that position was also a significant predictor of proportional landings (Likelihood ratio test:  $\chi^2[5] = 13.96$ ;  $P = 0.0158$ ). Position vi exhibited significantly lower proportional landings than positions i, ii and iii, indicative of positional bias (Figure S5C).

To support these findings under a nonparametric framework, we applied a permutation analysis as described above and found that several pairs of humans have landing percentage differences that are highly unlikely to be the result of a position bias alone (Figure 6D), thus confirming that participant identity drives landing preferences. This analysis once again confirmed that Human 3 was the most attractive individual and Human 2 showed the lowest level of attractiveness (Figure 6D). Furthermore, we discerned body weight across this six-person cohort did not correlate well with human attractiveness, suggesting that ratio-specific chemical constitution of human body odor, rather than overall body mass, is the primary driver of *An. gambiae* olfactory preference for certain humans over others (Figure S4D). In these six-person preference trials, mean wind speeds were also low (Figure S5D).

These data indicate that despite high levels of variability in landing activity (Figure S4C) and differences in environmental conditions (Figure S6) during nightly trials, our multi-choice sensory preference assay format is an efficient and powerful method to screen for humans at both ends of the attractiveness spectrum who are differentially attractive to *An. gambiae* relative to other individuals.

### **Integrative use of whole body odor volatilomics identifies candidate volatile organic compounds modulating human attractiveness to *An. gambiae***

To identify candidate chemical features of human scent modulating attractiveness to *An. gambiae*, we concurrently performed whole body volatilomics during the same six-human olfactory preference trials (Figure 7). To do this, we collected whole body odor from each human subject for chemical analysis by sampling air from the tents onto thermal desorption tubes containing the chemical sorbent Tenax-TA. Air sampling from all subject tents occurred simultaneously during the first 45 min of human occupancy. Odor was collected onto the thermal desorption tubes by inserting them into a pump placed into the output ducting from each tent, after the ducting fan assembly (Figure S4A). Samples were then analyzed by thermal desorption-gas chromatography/mass spectrometry (TD-GC/MS) to produce nightly chemical profiles of each human, resulting in a total of 36 human odor profiles (six individual human whole body odor signatures for six replicate nights) across the entire cohort throughout the study (Figure 7A).

In total, 1,057 individual chemical features were detected across this dataset, predominantly consisting of human volatiles released via the skin and breath of participants, exogenous contaminants from the tents and ducting, and volatiles introduced into the tents from the external environment, as well as features of unknown chemical identity due to limitations in current mass spectral libraries and standards for identification. All features in this dataset were initially used to generate a partial least squares discriminant analysis (PLS-DA) model (Figure 7B) to visualize variation between samples from each human subject and aid in the identification of features demonstrating significant variation.

We next leveraged our previous analysis of human whole body headspace<sup>2</sup> to target the primary chemical constituents of human whole body odor, confirming the identity of 40 known VOCs detected in whole body odor in this semi-field dataset (Data S2). Air-borne human odorants from numerous chemical classes were detected across subjects, including aldehydes, ketones, alcohols, carboxylic acids, and hydrocarbons. Of these identified compounds, 15 were found to exhibit substantial variation in the whole body emissions across the human cohort (Figures 7C and S7) including acetic acid, butyric acid, isobutyric acid, valeric acid, isovaleric acid, hexanoic acid, heptanoic acid, octanoic acid, nonanoic acid, decanoic acid, acetoin, geranylacetone, decanal, 1-dodecanol, and eucalyptol. These compounds were conserved in the skin and breath emissions of all participants (Figure 7A) but were released at different rates.

The majority of identified compounds differing between participants were carboxylic acids, which were generally more abundant as a class of molecules in the scent of Human 3 (the most attractive human subject) and least abundant in the scent of Human 2 (the least attractive human subject) (Figures 7C and S7). Specifically, Human 3 exhibited significantly higher abundances of the carboxylic acids butyric acid, isobutyric acid, and isovaleric acid, as well as the skin microbe-generated volatile acetoin (3-hydroxy-2-butanone) relative to all other human subjects (Figures 7C and S7). Conversely, Human 2 exhibited lower abundances of the vast majority of these 15 VOCs (Figures 7C and S7), including significantly lower abundances of the carboxylic acids butyric acid, isobutyric acid, valeric acid, isovaleric acid, acetic acid, hexanoic acid, heptanoic acid, nonanoic acid, and decanoic acid, as well as the aldehyde decanal, the monoterpene ketone geranylacetone and the saturated fatty alcohol 1-dodecanol (Figures 7C and S7). A notable exception was the monoterpenoid eucalyptol, which was significantly elevated by 3-fold in abundance in this individual relative to all others (Figure 7C).

These data indicate that despite nightly variation in chemical signatures of whole body odor between human subjects, a number of volatile organic compounds were consistently released at greater or lower concentrations by individuals demonstrated to be at either end of the attractiveness spectrum in this targeted cohort of six humans. Integrative use of this multi-choice olfactory preference assay with whole body volatilomics has therefore revealed candidate chemical modulators of human attractiveness to *An. gambiae*, including potential roles for air-borne carboxylic acids, the skin microbe-generated compound acetoin, and monoterpenoid eucalyptol as key olfactory cues modulating intra-specific host preference during the mosquito hunt for humans.

## DISCUSSION

The African malaria mosquito is a highly anthropophilic mosquito species that blood feeds preferentially on humans,<sup>42–45</sup> exhibiting an innate olfactory preference to seek out human body odor. In addition to displaying strong inter-specific host preference for the scent of humans over other vertebrate host animals,<sup>46</sup> *An. gambiae* has also been observed to consistently exhibit intra-specific host preferences to seek out and blood feed on certain humans over other individuals<sup>18–23</sup>—dangerous behaviors that promote the spread of malaria.<sup>17,24</sup> Volatile olfactory cues, including CO<sub>2</sub> and other human body odorants, as

well as thermal and visual cues have been demonstrated to play a critical role in driving close-range attraction of mosquitoes to hosts via multi-sensory integration.<sup>6–14</sup> In contrast, the role that human body odor plays at enlarged naturalistic spatial scales in this sensory processing strategy to steer host selection in a complex sensory environment typical of human habitation is less well understood.

We initially performed nighttime assays of *An. gambiae* host-seeking behavior within a laboratory context to gain further insight into the logic of multi-sensory integration at close range. Consistent with previous reports,<sup>6–8,47</sup> we determined that CO<sub>2</sub> strongly synergizes with heat to trigger mosquito landings in this small-scale arena (0.027 m<sup>3</sup>). At this close range, we also determined that CO<sub>2</sub> and heat alone elicited sustained low levels of mosquito landings on the infrared-illuminated, black, high-contrast target that we engineered. Wind tunnel experiments have shown that a high-contrast object in the presence of human foot odor and CO<sub>2</sub> can elicit elevated landing behavior from *Anopheles coluzzii* females under low-light conditions.<sup>9</sup> In an orthologous fashion, CO<sub>2</sub> stimulation has been shown to synergistically trigger attraction to warmth<sup>6–8</sup> and dark, high-contrast visual features in the yellow fever mosquito *Aedes aegypti*.<sup>8,10–13,47</sup>

In subsequent multi-choice preference assays within our 1,000 m<sup>3</sup> behavioral arena in Zambia, we similarly observed that female *An. gambiae* display strong behavioral preferences to land on 35°C targets when they are baited with CO<sub>2</sub> emissions reflective of a large human over background atmospheric air. Within this context however, heat alone was insufficient to elicit mosquito landings on these targets. Whether detection of CO<sub>2</sub> is required to trigger landing behavior on targets mimicking human skin temperature, or this gas simply guides mosquitoes to the proximity of a heat source to evoke landings, are outstanding questions.<sup>48</sup> In this study a single concentration of CO<sub>2</sub> (i.e. 400 ppm above background levels) was used to reflect the diluted CO<sub>2</sub> emissions observed at the output of the stimulus ducting from a human weighing ~100 kg. Future studies evaluating the effect of varying CO<sub>2</sub> concentration on mosquito olfactory preference is therefore an area for further research.

While at close range we observed that heat alone can elicit low levels of *An. gambiae* landing behavior on a 35°C black target situated on a white background in the lab, we did not observe any landings on the same infrared-illuminated, 35°C black targets situated on black containers arrayed within the semi-field cage arena in the absence of olfactory cues, such as CO<sub>2</sub> alone or whole body odor. It is possible that a lack of contrast between the semi-field version of the landing platform and its surrounds did not provide a strong enough visual cue, and as such the role of visual contrast should further be interrogated in semi-field studies. Such experiments could employ higher contrast between the platform and the background, as well as evaluating the effect of moonlight and cloud coverage on lighting conditions and associated mosquito behavioral responses.

Due to the high volatility of CO<sub>2</sub> and its long-range dissipation downwind from hosts in odor plumes,<sup>16</sup> it is likely that mosquitoes may initially track upwind along plumes of CO<sub>2</sub> via odor-guided optomotor-mediated positive anemotaxis,<sup>49</sup> while synergistically integrating detection of this gas with other human odorants of varied volatility as they

navigate closer toward a human host.<sup>14,50</sup> Eventually, once in proximity to humans, they may then encounter visual and heat cues emitted by the human body which are critically integrated with this suite of odor cues<sup>6,10,11,13,51</sup> to evoke mosquito landing behavior.

Although it is well known that the lower extremities, including the ankles and feet of humans, and their associated odors are highly attractive to *An. gambiae*, this mosquito species distributes randomly along the lower margins of the body adjacent to the ground when humans lay down—including the head, trunk, arms, and legs.<sup>52,53</sup> This suggests that convection currents play a primary role in dictating preferred biting sites for *An. gambiae* and this malaria vector may more broadly track odorants from the entire human body in combination with convection currents to evoke context-specific landing on certain humans—highlighting the importance of studying whole human body odor when assessing olfactory preferences.

When we tested olfactory preferences in a six-choice setting we found that mosquitoes showed an innate preference for certain humans despite navigating in a complex sensory environment with multiple sources of host odor. Strikingly, using air sampling and whole body volatilomics, we discerned that the majority of human body odorants found to significantly differ in abundance from the scent of humans innately preferred at both ends of the attractiveness spectrum were carboxylic acids. Carboxylic acids are introduced into human body odor via skin sebaceous glands and microbiota.<sup>54</sup> Specifically, we discerned that butyric, isobutyric, and isovaleric acids were significantly enriched in the most attractive subject, while these latter two carboxylic acids were significantly diminished alongside several other carboxylic acids in the least attractive of humans from this six-person cohort. Future studies with larger human cohorts will be crucial to further validate the role of these compounds in driving differential attraction to humans in naturalistic contexts. Integrative use of complementary mosquito attraction assays, such as human landing catches and exposure-free human-baited double net traps,<sup>18,19,22,55</sup> may further be employed in competition inside our semi-field arena to independently validate rankings in attractiveness derived from the multi-choice system described here.

In a recent study examining the attractiveness of arm odor from different humans to *Ae. aegypti*, contact-based sampling was used to show that highly attractive individuals had increased abundances of a number of medium and long-chain carboxylic acids (C<sub>10</sub>–C<sub>20</sub>).<sup>56</sup> Additional contact-based sampling in a laboratory study ranking human attractiveness to *An. gambiae* has similarly revealed that the carboxylic acids lactic acid, 2-methylbutanoic acid, and tetradecanoic acid were highly enriched in foot odor from attractive individuals.<sup>37</sup> We observed similar trends in our study using air sampling with whole body odor under semi-field conditions, with the exception that we detected more highly volatile carboxylic acids (C<sub>2</sub>–C<sub>10</sub>), with these being more or less abundant in whole body odor of human subjects at both ends of the attractiveness spectrum. Our analysis therefore advances upon these important studies that used contact-based sampling, yielding fundamental insights into carboxylic acids with higher volatility that may guide attraction of *An. gambiae* toward humans from a distance.

The skin-microbe-generated compound acetoin (3-hydroxy-2-butanone) was also highly enriched in the most attractive human subject in the six-choice trial. Acetoin is amongst the most abundant of VOCs detected in the human whole body volatilome.<sup>2</sup> The bacteria *Staphylococcus epidermidis* and *Staphylococcus aureus* have been demonstrated to produce acetoin, both of which populate human skin.<sup>29,57–59</sup> The role of acetoin in mosquito host-seeking has not been well studied, although some evidence does suggest this compound may be implicated in *An. gambiae* attraction to humans.<sup>60</sup>

An important area for future research will thus be to leverage our semi-field system with expanded cohorts of humans to understand the role of inter-individual variability in the human skin microbiome<sup>58,59</sup> on VOC production and associated attractiveness. Reconstitution of synthetic blends containing these components and other conserved human odorants may be further used to test their sufficiency to evoke mosquito olfactory attraction. Such studies may have the potential to yield blends that are super attractive to *An. gambiae* and other anthropophilic disease vectors for enhanced vector surveillance and control by mimicking the chemistry of scent signatures from highly attractive humans.

In contrast, just as the presence of specific attractant cues in human odor may lead to an increase in human attractiveness to mosquitoes, the presence of repellent volatile compounds may have the opposite effect. Interestingly, the monoterpenoid eucalyptol (1,8-Cineole) was highly abundant in the body odor of the least preferred human subject in the six-person cohort. This compound is likely derived from plant-based foods and flavorings in diets, with humans being estimated to consume on average 4.5 mg daily, and is also a common additive in exogenous products.<sup>61</sup> Eucalyptol is a molecule with known mosquito repellency<sup>62–64</sup> and deodorizing action<sup>65</sup> that has been frequently detected in the skin and breath emissions of humans.<sup>66</sup> Noticeably, in addition to general depletion of carboxylic acids, several other compounds including decanal, geranylacetone, and 1-dodecanol had low relative abundances in the whole body odor of the least attractive individual. Whether this is due to an inherent low abundance of these compounds or a masking effect associated with the high levels of eucalyptol remains to be characterized in a larger screen of participants. Expansion of the behavioral screens described here to identify individuals whose scent is consistently not attractive to mosquitoes when placed in competition with others may therefore have the potential to reveal both established and novel biomarkers of human repellency to mosquitoes.

In summary, this study reveals that under naturalistic conditions human scent guides mosquito thermotaxis and host selection in *An. gambiae*. Our findings illuminate signature features of the human volatilome including key volatile carboxylic acids, the skin-microbe derived compound acetoin, and the monoterpenoid eucalyptol, among others, with potential to drive heterogeneity in human attractiveness to this prolific malaria vector. By extension, the comparative power of the multi-choice preference assay that we have developed here for use under naturalistic semi-field conditions in Zambia could readily be used to study how factors such as diet, pregnancy, the human microbiome, and infectious state drive preferential attraction of diverse malaria vectors to humans and define the chemosensory basis of malaria transmission at high definition.

## STAR★METHODS

### RESOURCE AVAILABILITY

**Lead contact**—Further information and requests for resources and reagents should be directed to and will be fulfilled by the lead contact, Conor McMeniman (cmcmeni1@jhu.edu).

**Materials availability**—This study did not generate new unique reagents.

#### Data and code availability

- All raw data supporting these analyses has been deposited publicly in the Johns Hopkins Research Data Repository at <https://doi.org/10.7281/T1/IVVFCM>.
- All data were processed and analyzed using custom scripts, publicly available at <https://github.com/GordusLab/Giraldo-Rankin-Turner-Corver-et-al-2023>.
- Any additional information required to reanalyze the data reported in this paper is available from the lead contact upon request.

### EXPERIMENTAL MODEL AND STUDY PARTICIPANT DETAILS

**Mosquito strains and maintenance**—Laboratory experiments at Johns Hopkins Malaria Research Institute (JHMRI) were performed with the *Anopheles gambiae* Keele strain. Mosquitoes were maintained with a 12hr light:dark photoperiod at 27°C and 80% relative humidity using a standardized rearing protocol. Adults were provided with a 10% sucrose solution for colony maintenance.

Semi-field system experiments at Macha Research Trust, Zambia (MRT) were performed with the *Anopheles gambiae* Kisumu strain. Mosquitoes were laboratory reared in an insectary facility adjacent to the flight cage. Mosquitoes were maintained with a natural light:dark cycle at 26°C–30°C and 70%–80% relative humidity using a standardized rearing protocol. Adults were provided with a 6% glucose solution for colony maintenance.

**Human participants**—A total of 7 participants were recruited for this study, all healthy adults aged 18 years and older. These consisted of 5 males and 2 females. 5 participants were Black (4 males and 1 female), 1 participant was Hispanic or Latino (1 male), and 1 participant was white (1 female). Socioeconomic status of all participants was medium. Recruitment of the cohort was based on availability of participants and sex was not a factor taken into consideration during data analysis due to the small cohort size. Informed consent was obtained from all participants. This study was approved by the Johns Hopkins Bloomberg School of Public Health (JHSPH) Institutional Review Board (IRB no. 00018691), Macha Research Trust (MRT) Institutional Review Board (IRB no. E.2021.06) and the National Health Research Authority of Zambia (NHRA0000004/08/04/2022).

### METHOD DETAILS

**Odor-guided thermotaxis assay**—An odor-guided thermotaxis assay (OGTA) was engineered in a 30 cm × 30 cm × 30cm cage (Bugdorm-1 Insect Rearing Cage, MegaView



Science Co.). The assay consisted of a heated platform placed on the floor of the cage, made from a black aluminum disk of 10cm in diameter with a Peltier element (Aideepen TEC1-12706) glued at the bottom. The Peltier element was controlled by an Arduino UNO microcontroller and a thermistor (WM222C, Sensor Scientific, Inc.) to keep the temperature at 35°C, mimicking human skin temperature. Surrounding the platform was a 3D printed ring with 12 infrared LEDs (840nm) powered by the Arduino to illuminate mosquitoes landing on the platform. A Raspberry Pi camera module (Camera Module 2 Pi NoIR) was placed on top of the cage to record mosquito activity and all recordings were carried out at 10fps. 5% percent CO<sub>2</sub> or clean synthetic air (Airgas) were brought into the cage with 1/4" vinyl tubing (Cole Parmer 06405-02), that was placed immediately adjacent to the platform in a set position, at a flow rate of 2 mL/s. The CO<sub>2</sub> pulses increased the concentration 1000 ppm above background levels.<sup>6</sup> All CO<sub>2</sub> concentrations in this study were measured with an IAQ Mini CO<sub>2</sub> meter (RAD-0302). The end of the tubing was capped with mesh to prevent mosquitoes from flying into it.

**Odor-guided thermotaxis assay under laboratory conditions**—Twenty-five mated and nulliparous *An. gambiae* Keele strain females (4–7 day old) were used for each replicate experiment at JHMRI to initially pilot the OGTA configuration prior to its adaptation for semi-field use. Approximately 30 h prior to experimentation, mosquitoes were cold anesthetized at 4°C, placed in a 3D-printed release trap, and provided with a 10% sucrose solution on a saturated wet cotton ball overnight. The sucrose solution was removed and replaced by a cotton ball soaked in dH<sub>2</sub>O the next day, 12 h prior to start of each experiment, to encourage host-seeking behavior.

Three or 4 h before the experiment, the release trap was placed in a fitted receptacle on the front of the OGTA cage and the assay placed in an isolated room maintained at 27°C and 60% humidity. In experiments using heat, the landing platform was warmed to 35°C to simulate human skin temperature. The platform was left unheated in no-heat experiments, but the temperature was monitored over the duration of the assay using the thermistor. For all experimental replicates, a paper towel wick was inserted into a round glass bottle (Fisherbrand FB02911944) containing dH<sub>2</sub>O that was placed in each assay to prevent mosquito desiccation throughout the night.

To initiate each experiment, the release trap was opened, and mosquitoes were allowed to freely move into the enclosure. All lights in the room were turned off except for two night lights (MAZ-TEK YOOUS, 25 lumens) placed on the floor in front of the OGTA resulting in a total light intensity of 0.04 lux to simulate nighttime partial moon conditions.<sup>38</sup> Mosquitoes were allowed to acclimate for 3–4 h before the start of the experiment to ensure that enough time passed since an experimenter was in the room, minimizing the possibility of human odors influencing mosquito behavior. At 20:00 hours mosquito landings on the platform were recorded for 30 min at 10fps. Five percent CO<sub>2</sub> or clean synthetic air was pulsed using a solenoid valve (Clippard ETO-3-12) and valve controller (Automate Scientific ValveLink 8.2) into the assay at the set position immediately adjacent to the platform at 20:00 hours and 20:15 hours for 1 min each at a flow rate of 2 mL/s. Mosquito landings were tracked using background subtraction algorithm with ivTrace (Jens P. Lindemann, Bielefeld University, <https://opensource.cit-ec.de/projects/ivtools/documents>).

All the trajectories were manually corrected using ivTrace's sort feature. The resulting file from ivTrace containing the trajectories was imported into MATLAB (The Mathworks Inc., R2018b) to quantify the number of landings and platform occupancy throughout time (i.e. every time a new object was detected). Full trajectories were obtained to discern when new mosquitoes landed on the platform as a high-content metric of attractiveness and preference.

**Semi-field system**—Semi-field experiments were performed in a custom flight cage facility (20 m L x 20 m W x 2.5 m H) constructed at Macha Research Trust, Chroma District, Southern Province, Zambia. The flight cage was positioned in a large open field on a gentle slope flanked at its margins by native foliage and grasses. A corrugated metal roof was installed on this facility to protect the central screened flight cage arena and enclosed assay components from weather-related damage due to the heavy seasonal rainfalls encountered in the Macha region during the wet season, which typically spans from November–April in Southern Zambia. An anteroom to facilitate secure entry and exit from the central flight cage arena was positioned on the northeastern side of the cage. Eight one-person tents (one-person Swag tent, #8101, Kodiak Canvas) were distributed evenly around exterior walls of the screened flight cage (two tents per side) to accommodate sleeping humans and other olfactory stimuli such as CO<sub>2</sub> that were introduced into them. For participant comfort and protection from inclement weather, tents were erected on stretchers (Outfitter XXL Camp Cot, #120A, Teton Sports) that were placed on dedicated concrete slabs, each 15m away from the perimeter of the central flight cage. To ensure that aluminum ducting piping olfactory stimuli from each tent into the flight cage were of uniform length and spatial position, each concrete tent slab was made to be level with the slab of the central flight cage arena. In a clockwise manner from the northeastern side of the cage, the tops of each pair of side tent slabs were 27cm and 23cm; 74cm and 95cm; 125cm and 120cm; and 30 cm and 8cm from the ground, respectively.

Each tent was modified using a ducting flange so that 4" air conditioning aluminum ducting could be connected to the front canvas surface of the foot of the tent. The tent was then connected to an inline fan (Inline Blower, Rule) powered by a 12V battery (12AH). Eight window access ports on the sides of the flight cage arena (two per side) allowed the 4" aluminum ducting from the tent fans to be connected to the cage. Inside the cage, each window access port was connected via ducting connectors to a modified version of the OGTA described above. The opening of the 4" ducting was secured in place in front of the platform using a U-bracket, and it was covered with aluminum screen to prevent mosquitoes from flying into it. The fan was used to duct air from the tents onto the OGTA at a speed of 0.8 m/s. Airflow at the output of the ducting on the OGTA was calibrated using a handheld anemometer (Testo 405i) and airflow adjusted by modifying fan speed using a pulse width modulator (RioRand RR-6-90V-15A-PSC). The mosquito landing platform was warmed to 35°C and illuminated with 12 infrared LEDs controlled by an Arduino, and mosquito landings were recorded with the video camera placed directly over the platform. The Raspberry Pi and Peltier element were powered by two 12V batteries, and all electronic components were placed in a black container that had the landing platform and infrared sensitive camera (Raspberry Pi Camera Module 2 NoIR) held by a camera stand (Myrin Korea B00AUJHKC2) on top of the container lid. Four water containers were placed in an

evenly spaced configuration in the corners and two wet towels were placed in the center of the flight cage to increase local humidity around the OGTA during assays.

**Mosquito preparation for semi-field behavioral experiments**—To prepare for each evening of assays in the semi-field system, 200 mated and nulliparous *An. gambiae* Kisumu strain females (laboratory reared and 3–5 day old) were aspirated into a 30 × 30 × 30 cm release cage (Bugdorm-1 Insect Rearing Cage, MegaView Science Co.) at 8:00 hours and glucose starved for 12 h prior the start of experimentation. During glucose deprivation, mosquitoes were provided with wet cotton balls soaked with dH<sub>2</sub>O as a water source and maintained under insectary conditions with natural light conditions until the evening. Mosquitoes were released into the center of the flight cage at 20:00 hours and allowed to acclimate to semi-field conditions for 2 h. Release was performed by manual opening of the holding cage by an experimenter who promptly left the flight cage arena. Landing platforms were heated to 35°C and infrared LEDs on all platforms were switched on immediately before mosquito release at 20:00 hours and remained on for the entirety of the experiment. Mosquito activity on each platform was recorded at 10fps for the duration of the experiments, which occurred with varying lengths of duration depending on the experimental configuration between 22:00 hours and 4:00 hours (see below). Mosquitoes were collected and totally cleared from the cage every morning using mechanical aspiration (Prokopack 1419, John W. Hock Company).

**Preference for CO<sub>2</sub> versus environmental air**—To quantify *An. gambiae* olfactory preference for warmed targets baited with CO<sub>2</sub> relative to environmental air, eight OGTA were arrayed in an octagonal pattern in the center of the flight cage and heated to 35°C. A CO<sub>2</sub> stimulus of 400 ppm above background atmospheric concentrations was selected as a representative dose for semi-field experimentation to reflect the upper range of CO<sub>2</sub> emissions that we observed at the output of tent ducting with human volunteers. Previously, we determined using a whole body headspace collection chamber that CO<sub>2</sub> emissions linearly scale with human body size.<sup>2</sup> The representative CO<sub>2</sub> dose we used was informed by a pilot screen of four human subjects (2 females and 2 males), where mean CO<sub>2</sub> concentrations at the output of the tent ducting were 258 ppm above background, with a lower range of 143 ppm above background (from a 47.6kg female) and an upper range of 438 ppm above background (from a 110.8 kg male), respectively. We therefore chose 400 ppm above background as a representative dose to reflect CO<sub>2</sub> emissions from a large human with a weight of ~100 kg. To generate this dose, a 100% CO<sub>2</sub> source was introduced into a single tent using 1/4" tubing at a flowrate of 300 mL/min from a compressed tank using a tank regulator and flow meter for the entire duration of the experiment. This yielded a diluted CO<sub>2</sub> stimulus that was 400 ppm above background atmospheric CO<sub>2</sub> concentrations at the output of the ducting onto the OGTA after mixing with environmental air being drawn through the tent by the ducting fan assembly at rate of 0.8 m/s. CO<sub>2</sub> concentration at the output of OGTA ducting using these flow parameters was determined under simulated assay conditions in the laboratory using an identical tent configuration and ducting flow rate using a CO<sub>2</sub> meter (IAQ Mini, CO2Meter, USA). No stimulus was added to the seven remaining tents, and air from all tents was brought into the cage and onto the platforms at a speed of 0.8 m/s as described above. The CO<sub>2</sub> stimulus was inserted into a different tent every night

to control for possible position effects and experiments were carried out for 6 consecutive nights. Recordings were carried out for 6 h from stimulus onset at 22:00 hours to 4:00 hours. Mosquito trajectories were obtained using ivTrace (Jens P. Lindemann, Bielefeld University, <https://opensource.cit-ec.de/projects/ivtools/documents>) and the trajectories were manually corrected. Landings and platform occupancy were quantified with MATLAB as described above (The Mathworks Inc., R2018b).

**Preference experiments with humans**—For one-human experiments in 2020, one healthy adult male was used, while for two-human experiments in 2020, an additional healthy adult male was recruited. For six-human experiments in 2022, a new cohort of six healthy adults was recruited consisting of two new females, three new males and one of the males (Human 1) from the 2020 studies. Study participants in the two-human and six-human experiments were assigned random numerical identifiers, with the exception of male Human 1 who was assigned the same identifier across one-human, two-human and six-human experiments. Participants in the six-person cohort were provided with odor-free shampoo and body wash (Vanicream, USA) to wash with each day of the study prior to sampling. After washing, participants were requested not to use any other cleaning products, deodorants, fragrances or cosmetics. For 12 h prior to each experiment, participants were also asked to refrain from the consumption of alcohol and odorous foods such as onions and garlic. Prior to entering the tents, participants changed into a set of scrubs (65/35 polyester/cotton, SmartScrubs, Phoenix, USA) washed only in water to reduce the introduction of exogenous VOCs from non-standardized clothing. Clothing was not standardized during the one-person and two-person experiments as these occurred during an early pilot phase of assay development, prior to later recruitment of the six-person cohort after standardization of assay conditions.

**Preference for human whole body odor versus CO<sub>2</sub>**—To quantify *An. gambiae* olfactory preference for warmed targets baited with human whole body odor relative to CO<sub>2</sub>, a total of eight OGTA's heated to 35°C and associated tents were used. One male human subject slept in one tent over consecutive nights to provide a replicate human whole body odor stimulus. The CO<sub>2</sub> concentration used for these experiments was the same as described above. To achieve this concentration a 100% CO<sub>2</sub> source from a compressed tank was split equally to achieve a flow rate of 300 mL/min into each of the seven other tents, yielding a 400ppm CO<sub>2</sub> stimulus above background at the output of the ducting of each concordant OGTA after mixing with environmental air being drawn through each tent by the ducting fan assemblies. Air from the tents was brought into the cage and onto the platforms at a speed of 0.8 m/s as described above. To avoid position effects and prevent possible bias due to contamination of the tent and landing platform by human scent, the human subject together with the tent, ducting, and platform were rotated every night. This was to ensure the human would sleep in the same tent, but at different positions relative to the cage. The same person was tested over 6 six consecutive nights. Recordings were carried out from stimulus onset at 22:00 hours to 4:00 hours. Mosquito trajectories were obtained using ivTrace (Jens P. Lindemann, Bielefeld University, <https://opensource.cit-ec.de/projects/ivtools/documents>) and all the trajectories were manually corrected. Landings and platform occupancy were quantified with MATLAB as described above (The Mathworks Inc., R2018b).

**Preference between two humans**—To quantify *An. gambiae* olfactory preference for human whole body odor from two different humans, an assay configuration with eight OGTA and eight tents were used. Two male human subjects were placed in individual tents and no stimulus was added to the remaining tents. All eight platforms were heated to 35°C. Air from the tents was brought into the cage and onto all eight platforms at a speed of 0.8 m/s as described above. To avoid position bias, the position of the subjects was rotated relative to the cage as described for the human versus CO<sub>2</sub> experiments. Additionally, the position of human 2 relative to human 1 was changed every night until all possible combinations were tested over 7 consecutive nights. The same two people were tested every night. Recordings were carried out for 6 h from the moment the subjects entered the tent at 22:00 hours to 4:00 hours. Mosquito trajectories were obtained using ivTrace (Jens P. Lindemann, Bielefeld University, <https://opensource.cit-ec.de/projects/ivtools/documents>) and all the trajectories were manually corrected. Landings and platform occupancy were quantified with MATLAB as described above (The Mathworks Inc., R2018b).

**Preference between six humans**—To quantify *An. gambiae* olfactory preference for human whole body odor sourced from 6 different humans, an assay configuration with six OGTA and six tents was used. In these tests, OGTA were arranged in a hexagonal configuration with each unit spaced equidistantly 5.3 m from the two neighboring units. All OGTA were heated to 35°C and air from the tents was brought into the cage and onto the platforms at a speed of 0.8 m/s as described above. To avoid position bias, the position of the subjects was randomly rotated every night relative to the cage. Each subject slept in the same tent every night, but unlike previous experiments the platforms and ducting were maintained in the same position. Recordings started 21:30 hours to record landings in absence of a human stimulus. Humans were introduced at 22:00 h and recordings carried on until 1:00 hours for a total of 3.5 h. The same cohort of six subjects was tested over 6 replicate nights.

Given the high level of overall mosquito activity observed in six-human choice experiments, trajectories were calculated using a custom-made program on Python (Python 3.8.13) available at: <https://github.com/GordusLab/Giraldo-Rankin-Turner-Corver-et-al-2023>. Mosquito landing trajectories were reconstructed using a background-subtraction approach. Recording backgrounds were determined based on rolling windows of 5-min (3,000 frames) duration, with background intensities defined as the 15th percentile with respect to the time axis of each window. A background-subtracted pixel value ( $p_{i,j}$   $\in$  [0, 255]) was considered a region of interest relative to its corresponding background intensity ( $b_{i,j}$ ) if  $p_{i,j} \geq 1.25 * b_{i,j}$  and  $p_{i,j} - b_{i,j} \geq 25$ . Following erosion (2 iterations) and dilation (24 iterations), these regions of interest were stored in an intermediate MicroFlyMovieFormat representation to facilitate trajectory reconstruction and manual verification.

Mosquito landing trajectories were determined by linking previously identified bright pixel clusters across frames based on the euclidean distance between their centroid locations, with closer matches taking precedence. A maximum linking distance of 50 pixels was found to robustly identify trajectories. Trajectory frame ranges were considered to represent a landing if their velocity fell below 20 pixels/frame (“low velocity”), or if a timepoint occurred within a  $\leq 5$ -s window between two low-velocity periods. To ensure no false positive trajectory

detections occur due to background artifacts, trajectories with no significant displacement ( $\leq 20$  pixels span) were rejected. Furthermore, due to the occurrence of flickering of the infrared illumination on some recording days, we excluded putative trajectories that remained in a 20-pixel vicinity of bright background artifacts corresponding to areas of high illumination surrounding the LEDs. Maps of such light artifacts were defined as pixel locations whose 95th percentile (taken across frames) exceeded the overall 90th percentile of pixel intensities in all frames and positions. Landings and platform occupancy were quantified with MATLAB (The Mathworks Inc., R2018b).

**Human whole body volatilomics**—Whole body VOC samples were collected using low-power pumps (Pocket Pump, SKC Inc., USA) with attached sorbent tubes that were positioned inside the 4" diameter ducting transferring human odor from the tents. To facilitate sampling of air from the ducting in a closed fashion, pumps with attached sorbent tubes were placed within the sealed arm of a 4" diameter three-way ducting splitter (#KT18XH072, MyLifeUNIT) that was positioned 1m from the base of the tent downstream of the fan assembly. Pumps were positioned in this location, rather than at the output of the ducting on the OGTA platform, to avoid introduction of sound, heat and visual cues associated with these into the assay that could influence mosquito landing behavior. Whole body odor samples were collected directly onto Tenax-TA thermal desorption (TD) tubes (#020810-005-00, 6 × 60 mm, Gerstel, USA) at 250 mL/min<sup>-1</sup> for 45 min. Prior to sampling, TD tubes were conditioned at 300°C for 60 min in a stream of nitrogen at 50 mL/min<sup>-1</sup> using the Gerstel tube conditioner (TC2, Gerstel, USA) and then spiked with 40 ng of 4-methylphenol (99+%, TCI America, USA) as an internal standard. Whole body VOC sampling commenced at 22:00 hours each night upon entry of participants into the tents.

Samples were analyzed using thermal desorption gas chromatography/mass spectrometry (7890B GC, 5977N MSD, Agilent, USA). Tenax-TA tubes were placed in a Gerstel Thermal Desorption Unit mounted onto a Gerstel Cooled Injector System (CIS4) PTV inlet (Gerstel, USA). Analytes were desorbed in splitless mode starting at 30°C followed by an increase of 720°C/min to 280°C with a 3 min hold. Analytes were then transferred into the inlet which was held at -70°C and then heated at 720 °C/min to desorb analytes onto a HP-INNOWAX capillary column (30 m length x 0.25 mm diameter x 0.25 μm film thickness). The GC oven was programmed with an initial temperature of 40°C with a 2 min hold followed by an increase of 6°C/min to 250°C and held for 5 mins. A helium carrier gas with a flow rate of 1.2 mL/min<sup>-1</sup> was used. The MS analyzer acquired over a range of m/z 30–300 and was operated in EI mode. The transfer line and ion source were set to 250°C and 230°C respectively.

Raw data were converted to mzML formats using MSConvert version 3.0 and processed in MSDIAL version 4.90 for peak alignment, integration and deconvolution. MSDIAL parameters were as follows: average peak width 20 scans, smoothing level 3 scans, minimum peak height 1000, deconvolution sigma window 0.5, and EI similarity cutoff 70%. Chromatographic peaks occurring above the limit of detection were normalized to the internal standard. Identification of compounds was achieved by comparison of mass spectra with the NIST Mass Spectral Library version 2.2 and the MassBank of North America



spectral libraries and retention time matching with analytical reference standards (listed in the key resources table). MetaboAnalyst 5.0 was used for the production of heat maps and chemometric analysis.

**Weather data collection**—A weather station (HOBO U30 USB) was installed outside of the cage 12m away. Information on temperature, wind speed, wind gust, relative humidity and wind direction was collected every 10 min for the 2020 season and 15 min for the 2022 season. Weather data was analyzed with MATLAB (The Mathworks Inc., R2018b).

**Seasonality of mosquito behavioral assays**—All olfactory preference assays with laboratory-reared *An. gambiae* Kisumu strain in the semi-field system occurred during the wet season in Southern Zambia. Multi-choice OGTA trials with CO<sub>2</sub> emissions reflective of a large human versus environmental air, human whole body odor from one human versus CO<sub>2</sub> and human whole body odor sourced from two humans versus environmental air occurred during the period February/March 2020. Six-choice assays with a cohort of six humans occurred during the month of April 2022.

## QUANTIFICATION AND STATISTICAL ANALYSIS

Fisher's exact permutation tests were used to quantify statistical differences in landing percentages and total landings in laboratory OGTA experiments. The Benjamini-Hochberg procedure was used to correct for multiple comparisons (5% FDR).

For relative preference and total landing comparisons in semi-field experiments, we used a permutation test approach to evaluate the statistical significance of landing preferences for stimuli considering the potential for position bias in the flight cage arena. For each position, a landing percentage was computed relative to the total landing count on each day. Positional landing biases were defined as the mean (across days) of landing percentages by position. We simulated the null hypothesis that observed landing counts result only from such positional biases irrespective of stimulus by randomly re-assigning trajectories within a given experimental day to each of the positions, weighted according to the average position preferences (repeated 5,000 times). Statistical significance of paired comparisons was evaluated based on the probability of observing an average landing percentage difference or total landing difference under the null hypothesis that exceeds the experimentally observed differences. The Benjamini-Hochberg procedure was used to correct for multiple comparisons (5% FDR).

For 2-human experiments, a preference index was calculated as follows:

$$(\text{Landings human 1} - \text{Landings human 2}) / \text{Total landings}$$

A one-sample t test was used to calculate a significant difference from zero in the preference indices calculated.

For 6-human experiments where high variability in overall landing behavior and relative attractiveness across individuals between nights was observed, we used a generalized linear model framework to test the relationship between landings and various predictor variables.

Specifically, we fit a negative binomial regression model (with a log link function), defining the number of landings on a given position each night as the response variable, human and platform position as categorical predictor variables, and temperature and relative humidity as numeric predictor variables. The natural log of total landings on a given night was additionally included as an offset term, thereby effectively modeling the landings as proportions per night. By accounting for overdispersion, the negative binomial provided significantly better fit to the data than a Poisson model with identical structure (Likelihood ratio test:  $\chi^2[1] = 1198.3$ ;  $P < 1 \times 10^{-10}$ ). Estimated marginal means and pairwise contrasts among these estimated marginal means were computed with the “emmeans” package in R. To test the overall effect of human and position on landings, we compared the full model to reduced models that omitted each of these terms, respectively, using likelihood ratio tests. The model equation employed was as follows:

$$\log(E(\text{landings})) = \beta_0 + \beta_1(\text{humanh2}) + \beta_2(\text{humanh3}) + \beta_3(\text{humanh4}) + \beta_4(\text{humanh5}) + \beta_5(\text{humanh6}) \\ + \beta_6(\text{positionp2}) + \beta_7(\text{positionp3}) + \beta_8(\text{positionp4}) + \beta_9(\text{positionp5}) + \beta_{10}(\text{positionp6}) + \beta_{11}(\text{scale}(\text{relhumid})) + \beta_{12}(\text{scale}(\text{temp})) + \text{offset}(\log(\text{total\_landings}))$$

For volatilomic analyses of whole body scent signatures, partial least squares discriminant analysis (PLS-DA) was performed in Metaboanalyst 5.0 using all detected mass spectrometry features with data normalized by sum and autoscaled. Statistical differences in compound abundance were calculated using Fisher’s exact permutation tests. The Benjamini-Hochberg procedure was used to correct for multiple comparisons. This was performed with MATLAB (The Mathworks Inc., R2018b).

The number of replicates for each experiment is stated in its concordant figure legend. All numerical p values for multiple comparisons reported as letters in the figures can be found in Data S1.

## Supplementary Material

Refer to Web version on PubMed Central for supplementary material.

## ACKNOWLEDGMENTS

We thank Johns Hopkins Malaria Research Institute (JHMRI) and Bloomberg Philanthropies for generous funding to C.J.M. that supported this collaborative project with Macha Research Trust, Zambia (MRT). D.G. was supported by postdoctoral fellowships from the Human Frontier Science Program (LT000310/2019-L) and JHMRI. G.M.T received a postdoctoral fellowship from JHMRI. A.C. was supported by a graduate fellowship from the Kavli Neuroscience Discovery Institute. A.G. acknowledges funding from NIH (GM124883). We thank the JHMRI Insectary Core and Chris Kizito for *Anopheles gambiae* for lab assays; Ben Matthews for initial advice regarding infrared tracking; Marlys Book for assistance with tent modifications; Aliyah Silver for assistance with OGTA assembly; Julien Adam for drone photography; Lewis Kabinga, Pebble Moono, Saviour Simbeya, Clever Munsaka, Komana Siasikabole, Alpha Simudombe, Charlton Munsanje, Boyd Mulala and Steward Choli for assistance with the semi-field assays; the MRT entomology team for expert technical assistance and insectary support; the MRT workshop team for constructing the semi-field cage and all MRT staff for valuable logistical support.

## REFERENCES

- Gillies MT (1957). Age-groups and the biting cycle in *Anopheles gambiae*. A preliminary investigation. Bull. Entomol. Res 48, 553–559. 10.1017/S0007485300002728.

2. Rankin-Turner S, and McMeniman CJ (2022). A headspace collection chamber for whole body volatilomics. *Analyst* 147, 5210–5222. 10.1039/d2an01227h. [PubMed: 36260022]
3. Lindsay SW, and Snow RW (1988). The trouble with eaves; house entry by vectors of malaria. *Trans. R. Soc. Trop. Med. Hyg* 82, 645–646. 10.1016/0035-9203(88)90546-9. [PubMed: 3256125]
4. Kirby MJ, Green C, Milligan PM, Sismanidis C, Jasseh M, Conway DJ, and Lindsay SW (2008). Risk factors for house-entry by malaria vectors in a rural town and satellite villages in the Gambia. *Malar. J* 7, 2–9. 10.1186/1475-2875-7-2. [PubMed: 18179686]
5. Lindsay SW, Jawara M, Paine K, Pinder M, Walraven GEL, and Emerson PM (2003). Changes in house design reduce exposure to malaria mosquitoes. *Trop. Med. Int. Health* 8, 512–517. 10.1046/j.1365-3156.2003.01059.x. [PubMed: 12791056]
6. McMeniman CJ, Corfas RA, Matthews BJ, Ritchie SA, and Vosshall LB (2014). Multimodal integration of carbon dioxide and other sensory cues drives mosquito attraction to humans. *Cell* 156, 1060–1071. 10.1016/j.cell.2013.12.044. [PubMed: 24581501]
7. Corfas RA, and Vosshall LB (2015). The cation channel TRPA1 tunes mosquito thermotaxis to host temperatures. *Elife* 4, e11750. 10.7554/eLife.11750.001. [PubMed: 26670734]
8. Van Breugel F, Riffell J, Fairhall A, and Dickinson MH (2015). Mosquitoes use vision to associate odor plumes with thermal targets. *Curr. Biol* 25, 2123–2129. 10.1016/j.cub.2015.06.046. [PubMed: 26190071]
9. Carnaghi M, Belmain SR, Hopkins RJ, and Hawkes FM (2021). Multimodal synergisms in host stimuli drive landing response in malaria mosquitoes. *Sci. Rep* 11, 7379. 10.1038/s41598-021-86772-4. [PubMed: 33795798]
10. Alonso San Alberto D, Rusch C, Zhan Y, Straw AD, Montell C, and Riffell JA (2022). The olfactory gating of visual preferences to human skin and visible spectra in mosquitoes. *Nat. Commun* 13, 555. 10.1038/s41467-022-28195-x. [PubMed: 35121739]
11. Liu MZ, and Vosshall LB (2019). General visual and contingent thermal cues interact to elicit attraction in female *Aedes aegypti* mosquitoes. *Curr. Biol* 29, 2250–2257.e4. 10.1016/j.cub.2019.06.001. [PubMed: 31257144]
12. Barredo E, Raji JI, Ramon M, Degennaro M, and Theobald J (2022). Carbon dioxide and blood-feeding shift visual cue tracking during navigation in *Aedes aegypti* mosquitoes. *Biol. Lett* 18, 20220270. 10.1098/rsbl.2022.0270. [PubMed: 36166270]
13. Vinauger C, Van Breugel F, Locke LT, Tobin KKS, Dickinson MH, Fairhall AL, Akbari OS, and Riffell JA (2019). Visual-Olfactory Integration in the Human Disease Vector Mosquito *Aedes aegypti*. *Curr. Biol* 29, 2509–2516.e5. 10.1016/j.cub.2019.06.043. [PubMed: 31327719]
14. Dekker T, Geier M, and Cardé RT (2005). Carbon dioxide instantly sensitizes female yellow fever mosquitoes to human skin odours. *J. Exp. Biol* 208, 2963–2972. 10.1242/jeb.01736. [PubMed: 16043601]
15. Bidlingmayer WL, and Hem DG (1980). The range of visual attraction and the effect of competitive visual attractants upon mosquito (Diptera: Culicidae) flight. *Bull. Entomol. Res* 70, 321–342. 10.1017/S0007485300007604.
16. Zollner GE, Torr SJ, Ammann C, and Meixner FX (2004). Dispersion of carbon dioxide plumes in African woodland: Implications for host-finding by tsetse flies. *Physiol. Entomol* 29, 381–394. 10.1111/j.0307-6962.2004.00399.x.
17. Guelbéogo WM, Gonçalves BP, Grignard L, Bradley J, Serme SS, Hellewell J, Lanke K, Zongo S, Sepúlveda N, Soulama I, et al. (2018). Variation in natural exposure to anopheles mosquitoes and its effects on malaria transmission. *Elife* 7, e32625. 10.7554/eLife.32625. [PubMed: 29357976]
18. Lindsay SW, Adiamah JH, Miller JE, Pleass RJ, and Armstrong JR (1993). Variation in attractiveness of human subjects to malaria mosquitoes (Diptera: Culicidae) in The Gambia. *J. Med. Entomol* 30, 368–373. 10.1093/jmedent/30.2.368. [PubMed: 8459413]
19. Knols BG, de Jong R, and Takken W (1995). Differential attractiveness of isolated humans to mosquitoes in Tanzania. *Trans. R. Soc. Trop. Med. Hyg* 89, 604–606. [PubMed: 8594668]
20. Mukabana WR, Takken W, Coe R, and Knols BGJ (2002). Host-specific cues cause differential attractiveness of Kenyan men to the African malaria vector *Anopheles gambiae*. *Malar. J* 1, 17. 10.1186/1475-2875-1-1. [PubMed: 12513703]

21. Qiu YT, Smallegange RC, Van Loon JJA, Ter Braak CJF, and Takken W (2006). Interindividual variation in the attractiveness of human odours to the malaria mosquito. *Med. Vet. Entomol* 20, 280–287. 10.1111/j.1365-2915.2006.00627.x. [PubMed: 17044878]
22. Brady J, Costantini C, Sagnon N, Gibson G, and Coluzzi M (1997). The role of body odours in the relative attractiveness of different men to malarial vectors in Burkina Faso. *Ann. Trop. Med. Parasitol* 91, S121–S122. 10.1080/00034983.1997.11813252.
23. Himeidan YE, Elbashir MI, and Adam I (2004). Attractiveness of pregnant women to the malaria vector, *Anopheles arabiensis*, in Sudan. *Ann. Trop. Med. Parasitol* 98, 631–633. 10.1179/000349804225021307. [PubMed: 15324469]
24. Smith DL, McKenzie FE, Snow RW, and Hay SI (2007). Revisiting the basic reproductive number for malaria and its implications for malaria control. *PLoS Biol* 5, e42, 10.1371/journal.pbio.0050042. [PubMed: 17311470]
25. Ansell J, Hamilton KA, Pinder M, Walraven GEL, and Lindsay SW (2002). Short-range attractiveness of pregnant women to *Anopheles gambiae* mosquitoes. *Trans. R. Soc. Trop. Med. Hyg* 96, 113–116. [PubMed: 12055794]
26. Lindsay S, Ansell J, Selman C, Cox V, Hamilton K, and Walraven G (2000). Effect of pregnancy on exposure to malaria mosquitoes. *Lancet* 355, 1972. 10.1016/S0140-6736(00)02334-5. [PubMed: 10859048]
27. Verhulst NO, Beijleveld H, Knols BG, Takken W, Schraa G, Bouwmeester HJ, and Smallegange RC (2009). Cultured skin microbiota attracts malaria mosquitoes. *Malar. J* 8, 302. 10.1186/1475-2875-8-302. [PubMed: 20017925]
28. Verhulst NO, Qiu YT, Beijleveld H, Maliepaard C, Knights D, Schulz S, Berg-Lyons D, Lauber CL, Verduijn W, Haasnoot GW, et al. (2011). Composition of human skin microbiota affects attractiveness to malaria mosquitoes. *PLoS One* 6, e28991. 10.1371/journal.pone.0028991. [PubMed: 22216154]
29. Verhulst NO, Andriessen R, Groenhagen U, Bukovinszkiné Kiss G, Schulz S, Takken W, van Loon JJA, Schraa G, and Smallegange RC (2010). Differential attraction of malaria mosquitoes to volatile blends produced by human skin bacteria. *PLoS One* 5, e15829. 10.1371/journal.pone.0015829. [PubMed: 21209854]
30. Paskewitz S, Irwin P, Konwinski N, and Larson S (2018). Impact of consumption of bananas on attraction of *Anopheles stephensi* to humans. *Insects* 9, 129. 10.3390/insects9040129. [PubMed: 30274200]
31. Lefèvre T, Gouagna L-C, Dabiré KR, Elguero E, Fontenille D, Renaud F, Costantini C, and Thomas F (2010). Beer consumption increases human attractiveness to malaria mosquitoes. *PLoS One* 5, e9546. 10.1371/journal.pone.0009546. [PubMed: 20209056]
32. Shirai O, Tsuda T, Kitagawa S, Naitoh K, Seki T, Kamimura K, and Morohashi M (2002). Alcohol ingestion stimulates mosquito attraction. *J. Am. Mosq. Control Assoc* 18, 91–96. [PubMed: 12083361]
33. Lacroix R, Mukabana WR, Gouagna LC, and Koella JC (2005). Malaria infection increases attractiveness of humans to mosquitoes. *PLoS Biol* 3, e298. 10.1371/journal.pbio.0030298. [PubMed: 16076240]
34. Robinson A, Busula AO, Voets MA, Beshir KB, Caulfield JC, Powers SJ, Verhulst NO, Winskill P, Muwanguzi J, Birkett MA, et al. (2018). *Plasmodium*-associated changes in human odor attract mosquitoes. *Proc. Natl. Acad. Sci. USA* 115, E4209–E4218. 10.1073/PNAS.1721610115. [PubMed: 29666273]
35. Busula AO, Bousema T, Mweresa CK, Masiga D, Logan JG, Sauerwein RW, Verhulst NO, Takken W, and De Boer JG (2017). Gametocytemia and attractiveness of *Plasmodium falciparum*-infected Kenyan children to *Anopheles gambiae* mosquitoes. *J. Infect. Dis* 216, 291–295. 10.1093/infdis/jix214. [PubMed: 28859429]
36. Fernández-Grandon GM, Gezan SA, Armour JAL, Pickett JA, and Logan JG (2015). Heritability of attractiveness to mosquitoes. *PLoS One* 10, e0122716. 10.1371/journal.pone.0122716. [PubMed: 25901606]
37. Verhulst NO, Beijleveld H, Qiu YT, Maliepaard C, Verduyn W, Haasnoot GW, Claas FHH, Mumm R, Bouwmeester HJ, Takken W, et al. (2013). Relation between HLA genes, human skin volatiles

- and attractiveness of humans to malaria mosquitoes. *Infect. Genet. Evol* 18, 87–93. 10.1016/j.meegid.2013.05.009. [PubMed: 23688850]
38. Gaston KJ, Bennie J, Davies TW, and Hopkins J (2013). The ecological impacts of nighttime light pollution: A mechanistic appraisal. *Biol. Rev* 88, 912–927. 10.1111/brv.12036. [PubMed: 23565807]
  39. Degennaro M, McBride CS, Seeholzer L, Nakagawa T, Dennis EJ, Goldman C, Jasinskiene N, James AA, and Vosshall LB (2013). *orco* mutant mosquitoes lose strong preference for humans and are not repelled by volatile DEET. *Nature* 498, 487–491. 10.1038/nature12206. [PubMed: 23719379]
  40. Raji JI, Melo N, Castillo JS, Gonzalez S, Saldana V, Stensmyr MC, and DeGennaro M (2019). *Aedes aegypti* Mosquitoes Detect Acidic Volatiles Found in Human Odor Using the IR8a Pathway. *Curr. Biol* 29, 1253–1262.e7. 10.1016/j.cub.2019.02.045. [PubMed: 30930038]
  41. van Loon JJA, Smallegange RC, Bukovinszkiné-Kiss G, Jacobs F, De Rijk M, Mukabana WR, Verhulst NO, Menger DJ, and Takken W (2015). Mosquito attraction: crucial role of carbon dioxide in formulation of a five-component blend of human-derived volatiles. *J. Chem. Ecol* 41, 567–573. 10.1007/s10886-015-0587-5. [PubMed: 26026743]
  42. Garrett-Jones C, Boreham PFL, and Pant CP (1980). Feeding habits of anophelines (Diptera: Culicidae) in 1971–78, with reference to the human blood index: A review. *Bull. Entomol. Res* 70, 165–185. 10.1017/S0007485300007422.
  43. Pates HV, Curtis CF, and Takken W (2014). Hybridization studies to modify the host preference of *Anopheles gambiae*. *Med. Vet. Entomol* 28, 68–74. 10.1111/mve.12070. [PubMed: 25171608]
  44. Mwangangi JM, Mbogo CM, Nzovu JG, Githure JI, Yan G, and Beier JC (2003). Blood-meal analysis for anopheline mosquitoes sampled along the Kenyan coast. *J. Am. Mosq. Control Assoc* 19, 371–375. [PubMed: 14710739]
  45. Constantini C, Sagnon NF, della Torre A, and Coluzzi M (1999). Mosquito Behavioral Aspects of Vector-Human Interactions in the *Anopheles gambiae* complex. *Parasitologia* 41, 209–217.
  46. Dekker T, Takken W, and Braks MA (2001). Innate preference for host-odor blends modulates degree of anthropophagy of *Anopheles gambiae sensu lato* (Diptera: Culicidae). *J. Med. Entomol* 38, 868–871. 10.1603/0022-2585-38.6.868. [PubMed: 11761386]
  47. Kröber T, Kessler S, Frei J, Bourquin M, and Guerin PM (2010). An in vitro assay for testing mosquito repellents employing a warm body and carbon dioxide as a behavioral activator. *J. Am. Mosq. Control Assoc* 26, 381–386. 10.2987/10-6044.1. [PubMed: 21290933]
  48. Cardé RT (2015). Multi-cue integration: how female mosquitoes locate a human host. *Curr. Biol* 25, R793–R795. 10.1016/j.cub.2015.07.057. [PubMed: 26394099]
  49. Kennedy JS (1940). The visual responses of flying mosquitoes. *J. Zool A109*, 221–242.
  50. Dekker T, and Cardé RT (2011). Moment-to-moment flight manoeuvres of the female yellow fever mosquito (*Aedes aegypti* L.) in response to plumes of carbon dioxide and human skin odour. *J. Exp. Biol* 214, 3480–3494. 10.1242/jeb.055186. [PubMed: 21957112]
  51. Spitzen J, Spoor CW, Grieco F, ter Braak C, Beeuwkes J, van Brugge SP, Kranenbarg S, Noldus LPJJ, van Leeuwen JL, and Takken W (2013). A 3D Analysis of Flight Behavior of *Anopheles gambiae sensu stricto* Malaria Mosquitoes in Response to Human Odor and Heat. *PLoS One* 8, e62995–12. 10.1371/journal.pone.0062995. [PubMed: 23658792]
  52. Dekker T, Takken W, Knols BGJ, Bouman E, Laak S, Bever A, and Huisman PWT (1998). Selection of biting sites on a human host by *Anopheles gambiae s.s.*, *An. arabiensis* and *An. quadriannulatus*. *Entomol. Exp. Appl* 87, 295–300. 10.1046/j.1570-7458.1998.00334.x.
  53. Braack L, Hunt R, Koekemoer LL, Gericke A, Munhenga G, Haddow AD, Becker P, Okia M, Kimera I, and Coetzee M (2015). Biting behaviour of African malaria vectors: 1. Where do the main vector species bite on the human body? *Parasit. Vectors* 8, 76. 10.1186/s13071-015-0677-9. [PubMed: 25650005]
  54. Fredrich E, Barzantny H, Brune I, and Tauch A (2013). Daily battle against body odor: Towards the activity of the axillary microbiota. *Trends Microbiol* 21, 305–312. 10.1016/j.tim.2013.03.002. [PubMed: 23566668]
  55. Limwagu AJ, Kaindoa EW, Ngowo HS, Hape E, Finda M, Mkandawile G, Kihonda J, Kifungo K, Njalambaha RM, Matoke-Muhia D, and Okumu FO (2019). Using a miniaturized double-net trap

- (DN-Mini) to assess relationships between indoor-outdoor biting preferences and physiological ages of two malaria vectors, *Anopheles arabiensis* and *Anopheles funestus*. *Malar. J* 18, 282. 10.1186/s12936-019-2913-9. [PubMed: 31438957]
56. De Obaldia ME, Morita T, Dedmon LC, Boehmler DJ, Jiang CS, Zeledon EV, Cross JR, and Vosshall LB (2022). Differential mosquito attraction to humans is associated with skin-derived carboxylic acid levels. *Cell* 185, 4099–4116.e13. 10.1016/j.cell.2022.09.034. [PubMed: 36261039]
57. Fitzgerald S, Duffy E, Holland L, and Morrin A (2020). Multi-strain volatile profiling of pathogenic and commensal cutaneous bacteria. *Sci. Rep* 10, 17971. 10.1038/s41598-020-74909-w. [PubMed: 33087843]
58. Oh J, Byrd AL, Deming C, Conlan S, NISC Comparative Sequencing Program, Kong HH, and Segre JA (2014). Biogeography and individuality shape function in the human skin metagenome. *Nature* 514, 59–64. 10.1038/nature13786. [PubMed: 25279917]
59. Oh J, Byrd AL, Park M, NISC Comparative Sequencing Program, Kong HH, and Segre JA (2016). Temporal Stability of the Human Skin Microbiome. *Cell* 165, 854–866. 10.1016/j.cell.2016.04.008. [PubMed: 27153496]
60. Verhulst NO, Mbadi PA, Kiss GB, Mukabana WR, Van Loon JJA, Takken W, and Smallegange RC (2011). Improvement of a synthetic lure for *Anopheles gambiae* using compounds produced by human skin microbiota. *Malar. J* 10, 28. 10.1186/1475-2875-10-28. [PubMed: 21303496]
61. European Commission (2002). Health and Consumer Protection Directorate-General, Opinion of the Scientific Committee on Food on Eucalyptol.
62. Klocke JA, Darlington MV, and Balandrin MF (1987). 1,8-Cineole (Eucalyptol), a mosquito feeding and ovipositional repellent from volatile oil of *Hemizonia fitchii* (Asteraceae). *J. Chem. Ecol* 13, 2131–2141. 10.1007/BF01012562. [PubMed: 24301652]
63. Luo DY, Yan ZT, Che LR, Zhu JJ, and Chen B (2022). Repellency and insecticidal activity of seven Mugwort (*Artemisia argyi*) essential oils against the malaria vector *Anopheles sinensis*. *Sci. Rep* 12, 5337. 10.1038/s41598-022-09190-0. [PubMed: 35351963]
64. Maia MF, and Moore SJ (2011). Plant-based insect repellents : a review of their efficacy, development and testing. *Malar. J* 10, S11. [PubMed: 21411012]
65. Henmi A, Sugino T, Nakamura K, Nomura M, and Okuhara M (2020). Screening of deodorizing active compounds from natural materials and deodorizing properties of cineole. *J. Japan Assoc. Odor Environ* 51, 129–143. 10.2171/jao.51.129.
66. Drabi ska N, Flynn C, Ratcliffe N, Belluomo I, Myridakis A, Gould O, Fois M, Smart A, Devine T, and Costello BDL (2021). A literature survey of all volatiles from healthy human breath and bodily fluids: The human volatilome. *J. Breath Res* 15, 034001. 10.1088/1752-7163/abf1d0.



### Highlights

- Development of an expansive and naturalistic multi-choice smell test for mosquitoes
- CO<sub>2</sub> and other components of human scent guide *Anopheles gambiae* thermotaxis
- *Anopheles gambiae* exhibits olfactory preferences for some humans versus others
- Carboxylic acids are associated with human attractiveness to *Anopheles gambiae*

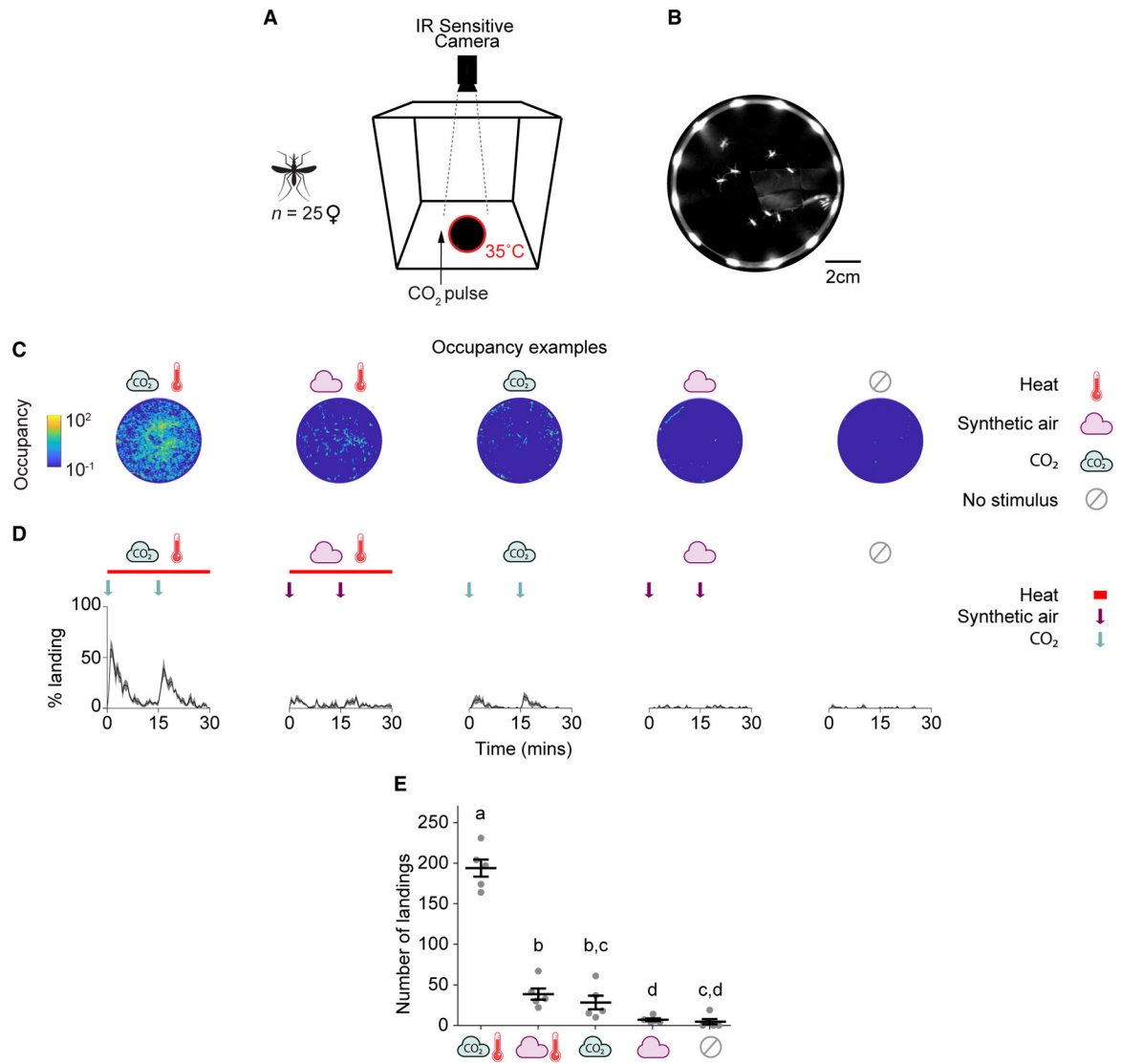


**Figure 1. OGTA for measuring *Anopheles gambiae* landing behavior at night**

(A) Schematic of the odor-guided thermotaxis assay (OGTA) for use in laboratory conditions. *An. gambiae* females (n = 25 per trial) were introduced into a cage containing a heated landing platform surrounded by infrared LEDs. CO<sub>2</sub> was puffed into the cage at t = 0 min and t = 15 min adjacent to the landing platform (arrow, 1 min per pulse) and mosquito landings were recorded.

(B) Example image frame of mosquitoes landing on the heated platform illuminated by the surrounding infrared light array.

(C) Heatmaps of platform occupancy from a representative experiment for each stimulus combination.

(D) Percentage of mosquitoes landing on the platform throughout the experiment for each stimulus combination. The arrows indicate the time points of stimulus onset. Bars represent the length of the heat stimulus duration. Mean ± SEM plotted.

(E) Total number of landings on the platform for each stimulus combination. Mean  $\pm$  SEM plotted.  $n = 5$ /stimulus combination. The letters indicate significant differences ( $p < 0.05$ ): Fisher's exact permutation tests with Benjamini-Hochberg correction. See also Data S1A.

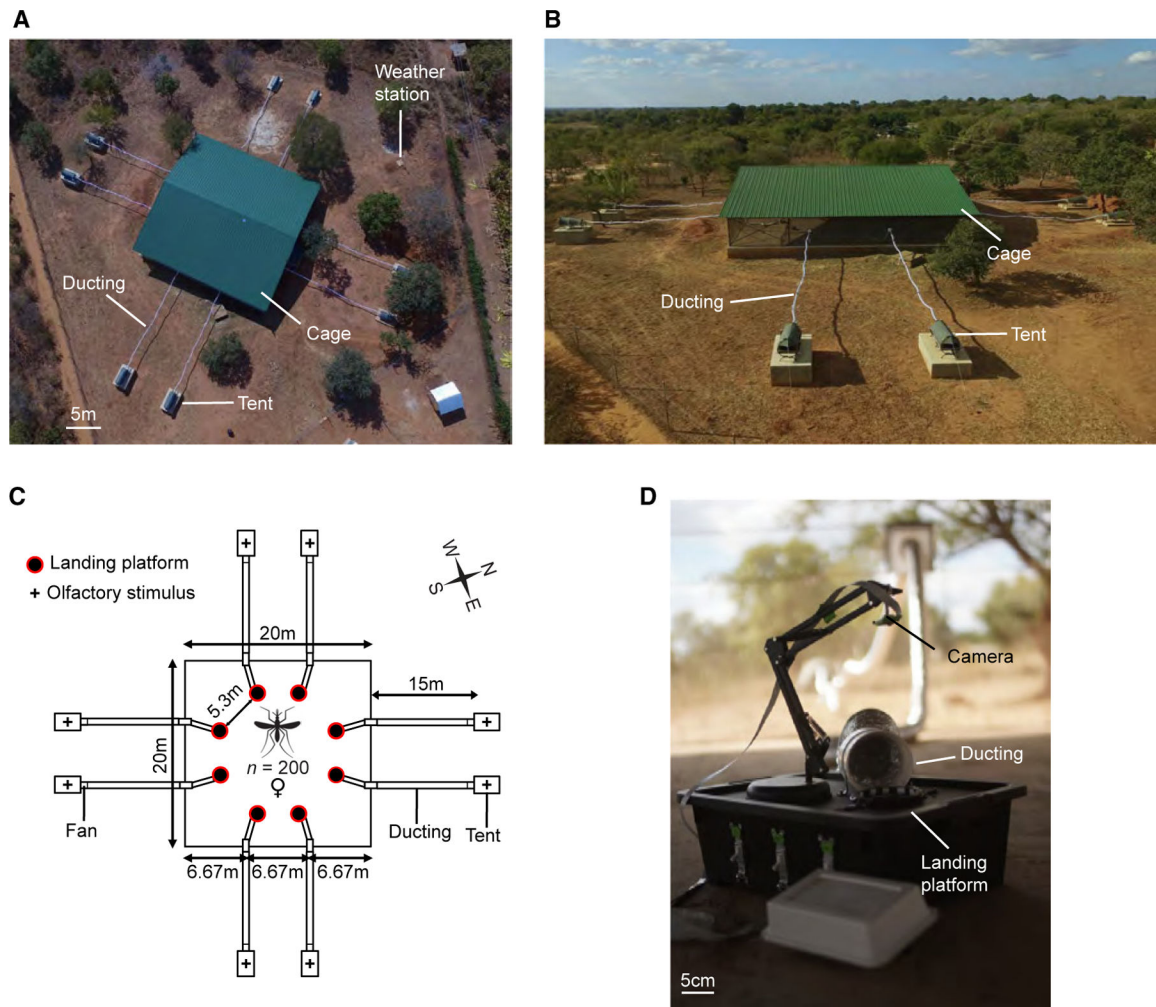


**Figure 2. Semi-field system for multi-choice assays of mosquito olfactory preference during host-seeking**

(A) Aerial view of the screened mosquito flight cage arena with roof (green) surrounded by 8 one-person tents. Tents (2 per side) are connected to deliver olfactory stimuli via a ducting fan assembly to the flight cage arena.

(B) Side view of the mosquito flight cage arena.

(C) Schematic of the multi-choice olfactory preference assay.  $n = 200$  mosquitoes per nightly trial.

(D) OGTA for use in the semi-field system. The ducting from each tent vents the target olfactory stimulus over a heated landing platform and mosquito landings are recorded. See also Figure S1.

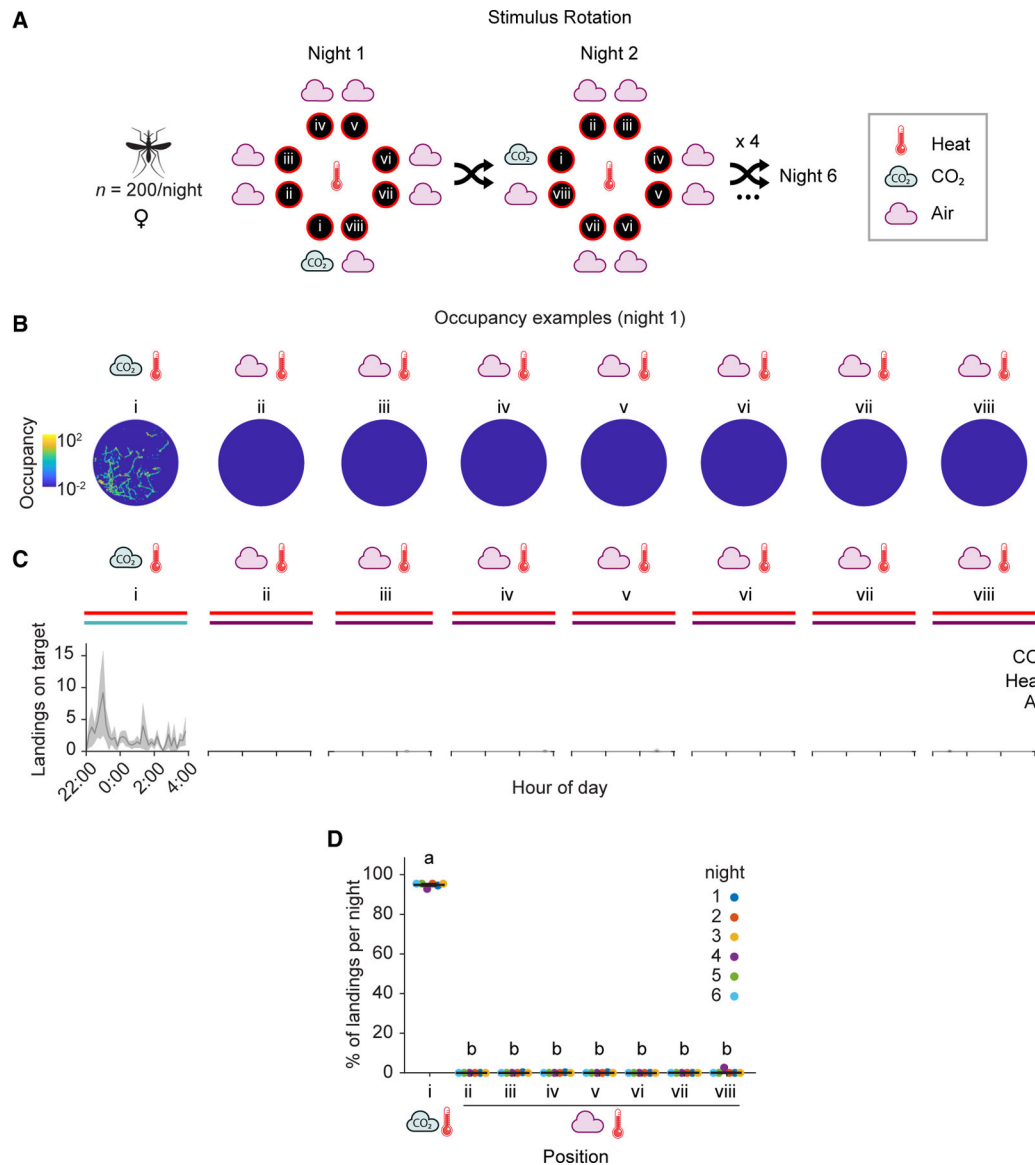


**Figure 3. *Anopheles gambiae* prefers to land on heated targets baited with CO<sub>2</sub> emissions reflective of a large human over background air**

(A) Stimulus position and rotation during eight-choice trials with these stimuli. The CO<sub>2</sub> stimulus (position i), 400 ppm above atmospheric concentrations to mimic the presence of a large human, was shuffled every night. The background air control positions (ii–viii) were labeled in reference to the CO<sub>2</sub> stimulus position in a clockwise manner. All platforms were heated to 35°C throughout the experiment.

(B) Heatmap of platform occupancy for an example night (night 1).

(C) Number of mosquito landings on the OGTA platforms throughout the experiment. Mean  $\pm$  SEM plotted.

(D) Percentage of the total landings per platform per night. Mean  $\pm$  SEM plotted.  $n = 6$  trials. The letters indicate significant differences ( $p < 0.001$ ): observed inter-individual mean landing percentage differences were compared (based on 5,000 permutation resampling

simulations) against the null hypothesis assuming these arise only from positional bias, with Benjamini-Hochberg correction.

See also Figures S1, S6, and Data S1B.

Author Manuscript

Author Manuscript

Author Manuscript

Author Manuscript



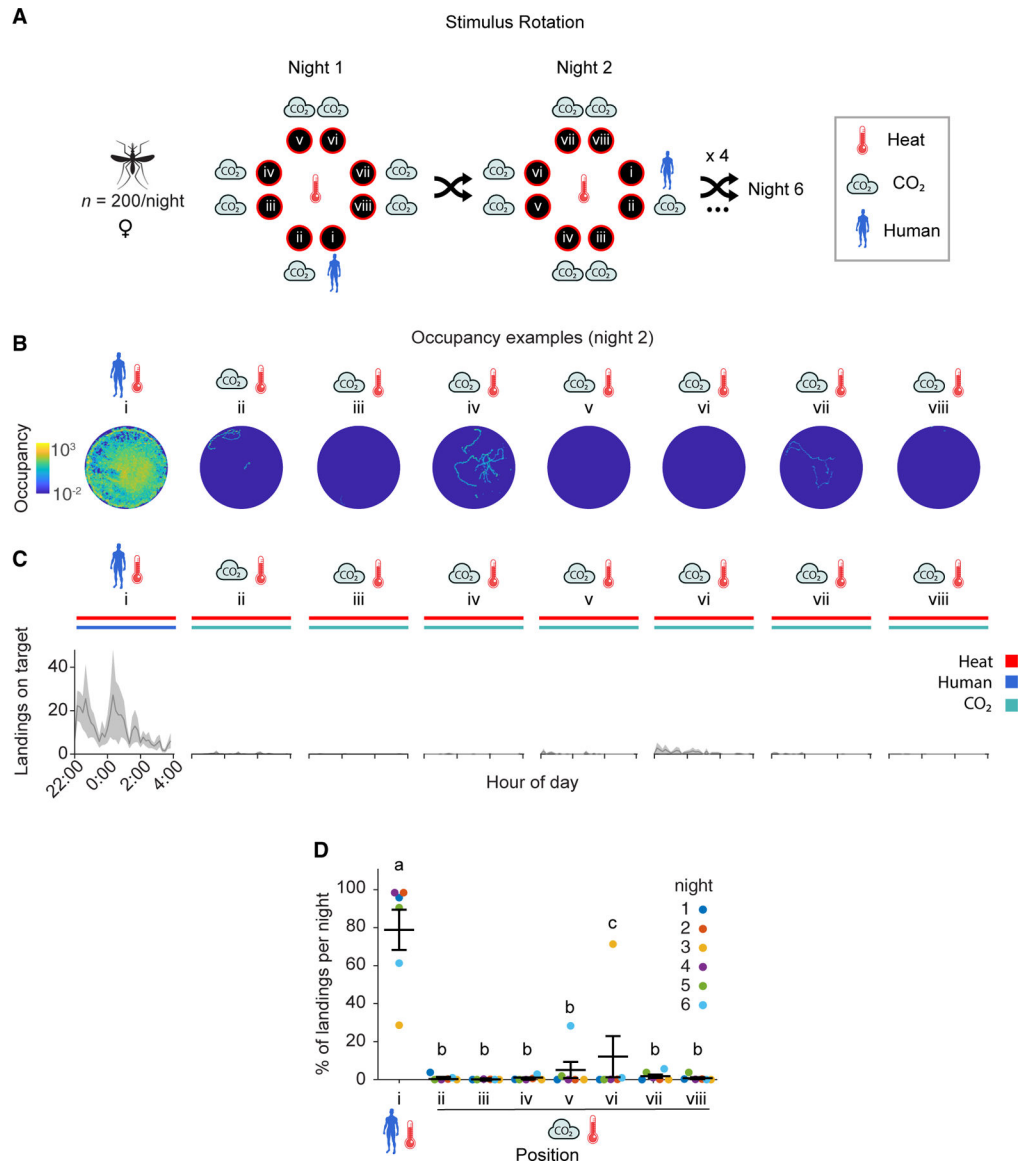


**Figure 4. *Anopheles gambiae* prefers to land on heated targets baited with the whole body odor of one human over CO<sub>2</sub> emissions reflective of a large human**

(A) Stimulus position and rotation during eight-choice trials with these stimuli. The human stimulus (position i) was shuffled every night. The remaining positions (ii–viii, CO<sub>2</sub>) were labeled in reference to the human position in a clockwise manner. All platforms were heated to 35°C throughout the experiment.

(B) Heatmap of platform occupancy for an example night (night 2).

(C) Number of mosquito landings on the OGTA platforms throughout the experiment. Mean  $\pm$  SEM plotted.

(D) Percentage of the total landings per platform per night. Mean  $\pm$  SEM plotted.  $n = 6$  trials. The letters indicate significant differences ( $p < 0.05$ ): observed inter-individual mean landing percentage differences were compared (based on 5,000 permutation resampling simulations) against the null hypothesis assuming these arise only from positional bias, with Benjamini-Hochberg correction.

See also Figures S2, S6, and Data S1C.

Author Manuscript

Author Manuscript

Author Manuscript

Author Manuscript

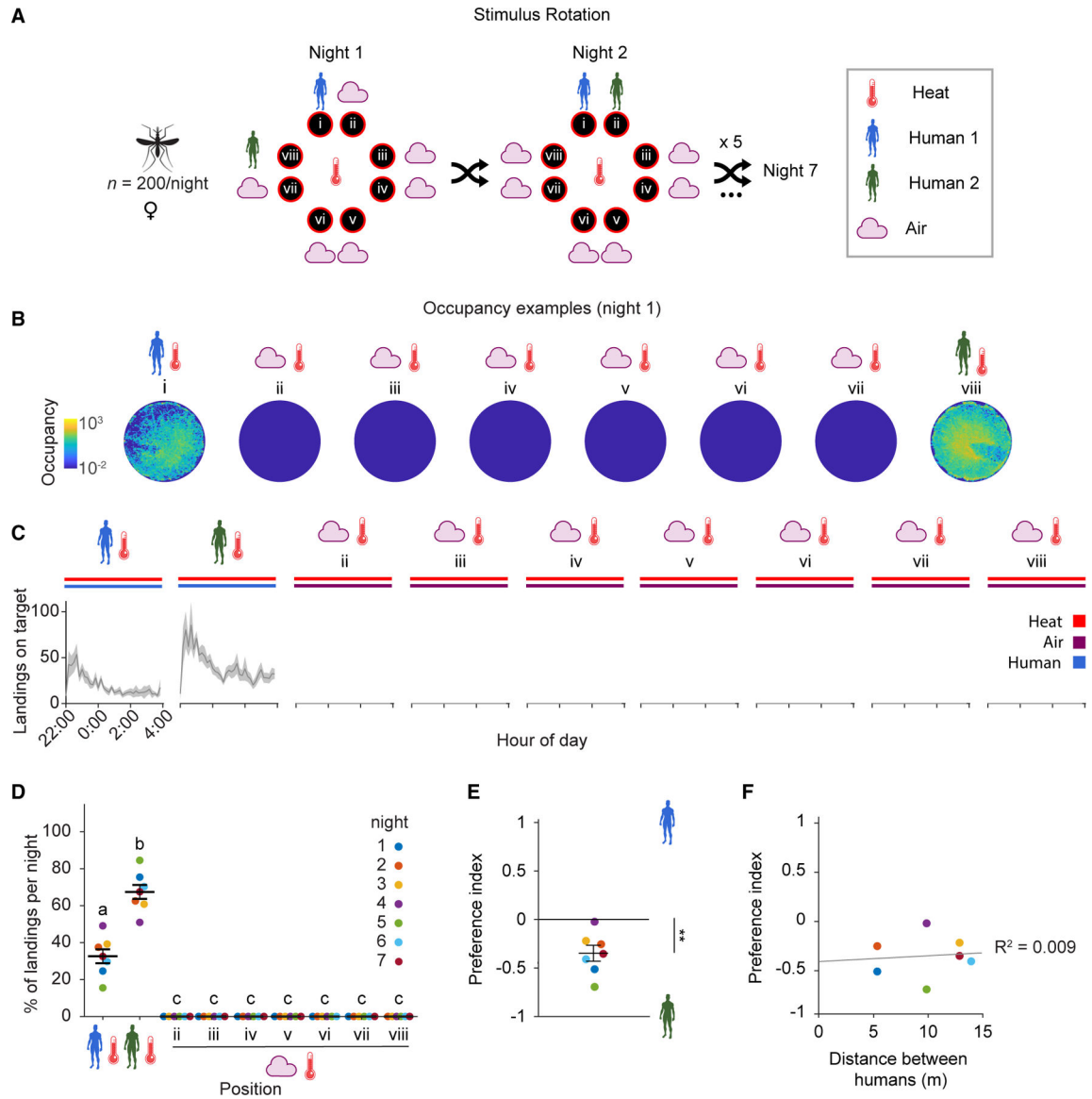


**Figure 5. *Anopheles gambiae* prefers heated targets baited with the body odor of one human over another**

(A) Stimulus position and rotation during eight-choice trials with whole body odor from two individual humans versus background air. The position of Human 1 (blue) and the position of Human 2 (green) relative to Human 1 were shuffled every night. The control positions (air) and the position of Human 2 were labeled in reference to Human 1. Human 2 could take any of the positions ii–viii.

(B) Heatmap of platform occupancy for an example night (night 1) where Human 2 took position viii.

(C) Number of mosquito landings on the OGTA platforms. Mean  $\pm$  SEM plotted.

(D) Percentage of the total landings per platform per night. Mean  $\pm$  SEM plotted.  $n = 7$  trials (control positions have 6 data points since one of the positions was occupied by Human 2 every night). The letters indicate significant differences ( $p < 0.05$ ): observed inter-individual mean landing percentage differences were compared (based on 5,000

permutation resampling simulations) against the null hypothesis assuming these arise only from positional bias, with Benjamini-Hochberg correction.

(E) Preference index calculated from total landings on Human 1 and 2. One sample t test for significant difference to 0:  $**p = 0.0054$ .

(F) Effect of distance between Human 1 and 2 on the preference index. Coefficient of determination  $R^2 = 0.009$ .

See also Figures S3, S6, and Data S1D.

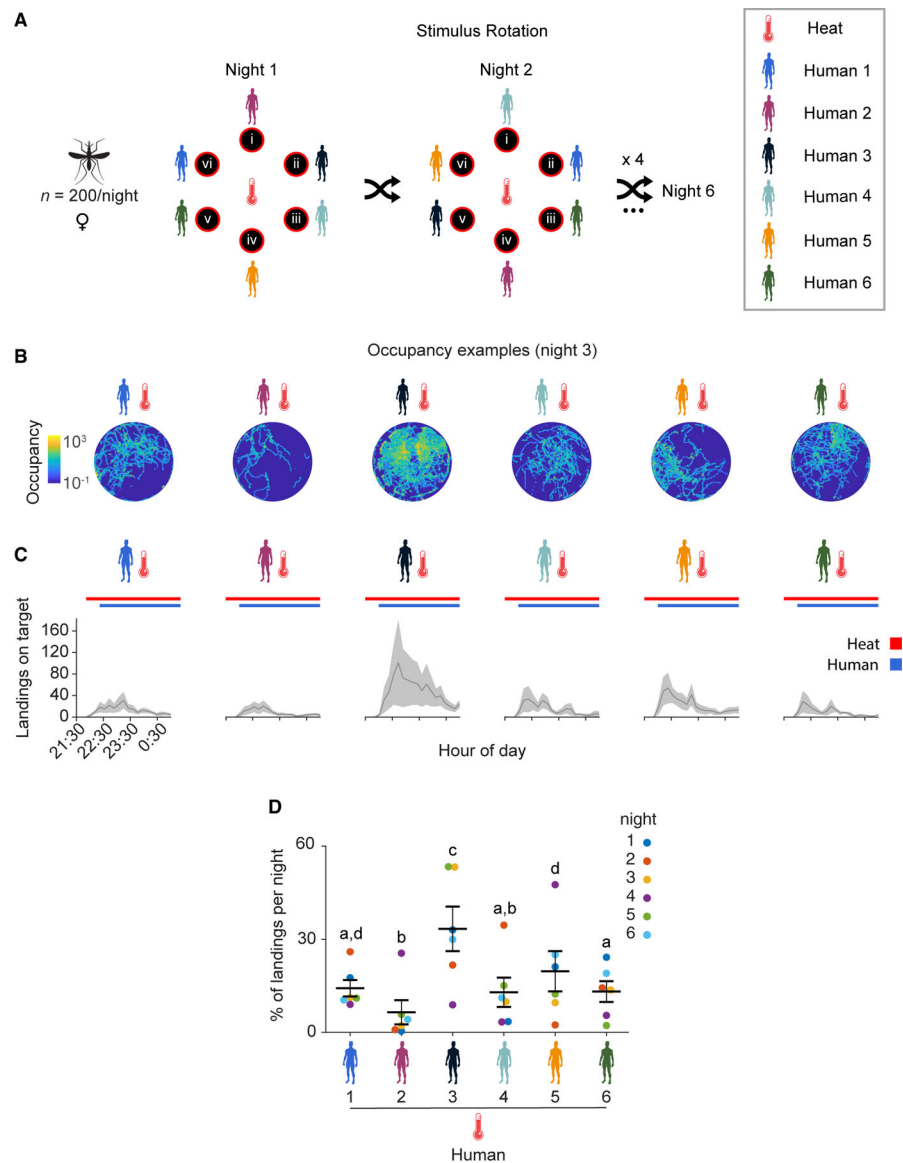


**Figure 6. *Anopheles gambiae* differentially prefers body odor from certain individuals in a six-choice context**

(A) Stimulus position and rotation during six-choice trials with six humans. Humans were shuffled randomly every night and could occupy any of the six positions (i–vi) numbered relative to their position in the cage.

(B) Heatmaps of platform occupancy for an example night (night 3).

(C) Number of mosquito landings on the platforms. Mean  $\pm$  SEM plotted.

(D) Percentage of the total landings per platform per night. Mean  $\pm$  SEM plotted.  $n = 6$  trials. The letters indicate significant differences ( $p < 0.05$ ): observed inter-individual mean landing percentage differences were compared (based on 5,000 permutation resampling simulations) against the null hypothesis assuming these arise only from positional bias, with Benjamini-Hochberg correction.

See also Figures S4, S5, S6, Table S1, and Data S1E.

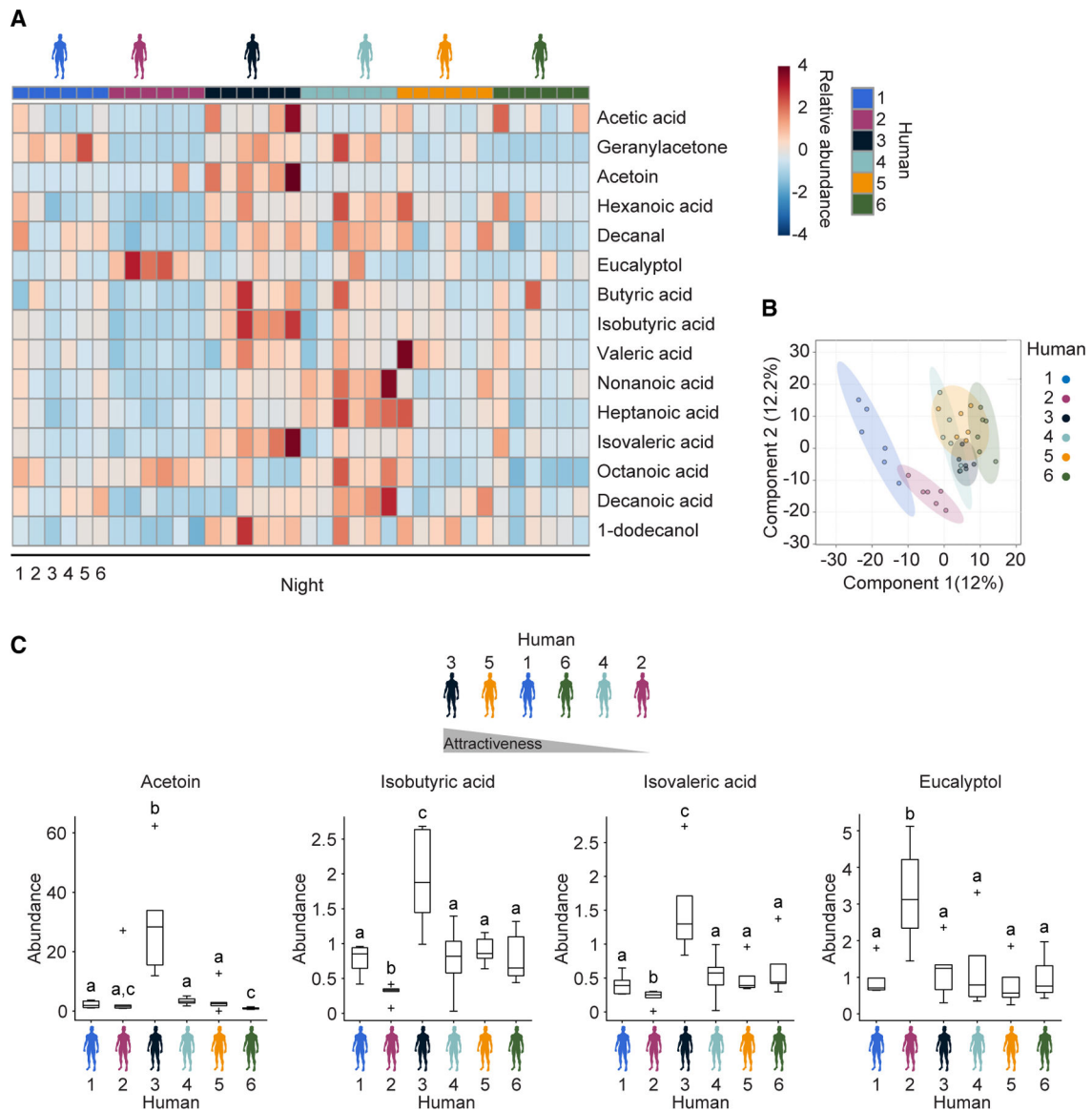


**Figure 7. Whole body volatilomics reveals candidate compounds modulating *Anopheles gambiae* olfactory preferences for human scent**

(A) Heatmap of 15 identified volatile organic compounds in human whole body odor demonstrating substantial variation between participants. Scale bar represents the amounts of analytes detected normalized to the internal standard, with red indicating a higher concentration and blue indicating lower concentration. Normalized across all participants. Heatmap constructed using MetaboAnalyst 5.0.

(B) PLS-DA score plot containing all chemical features detected. Ellipses indicate 95% confidence intervals. Plot constructed using MetaboAnalyst 5.0.

(C) Variation in 4/15 compounds of interest: acetoin, isobutyric acid, isovaleric acid, and eucalyptol detected in whole body odor from these humans. The line indicates the median, the box marks the lower and upper quartile, and the whiskers the 1.5 interquartile distance; outliers are indicated by black crosses. n = 6 trials. The letters indicate significant



differences ( $p < 0.05$ ) in compound abundance between humans: Fisher's exact permutation tests with Benjamini-Hochberg correction.  
See also Figure S7, Data S1F and S2.

Author Manuscript

Author Manuscript

Author Manuscript

Author Manuscript

## KEY RESOURCES TABLE

REAGENT or RESOURCE	SOURCE	IDENTIFIER
<u>Chemicals, peptides, and recombinant proteins</u>		
Synthetic clean air	Airgas	UZ300
5% CO <sub>2</sub>	Airgas	X02AI95C2000117
100% CO <sub>2</sub>	Afrox Zambia Ltd	40-RC
1-butanol (butan-1-ol)	Sigma Aldrich	B7906-500ML
1-dodecanol (dodecan-1-ol)	Sigma Aldrich	443816-500G
p-cresol (4-methylphenol)	TCI America	C0400
Acetic acid	Sigma Aldrich	338826-25ML
Acetoin (3-hydroxybutan-2-one)	Alfa Aesar	A13752
Acetophenone (1-phenylethanone)	Alfa Aesar	A12727
Alpha-pinene (2,6,6-trimethylbicyclo[3.1.1] hept-2-ene)	Sigma Aldrich	80605-1ML
Benzaldehyde	Sigma Aldrich	12010-250ML-F
Benzoic acid	Alfa Aesar	A14062
Benzothiazole (1,3-benzothiazole)	Acros Organics	146390050
Benzyl alcohol (phenylmethanol)	Sigma Aldrich	108006-100ML
Beta-caryophyllene ((1S,4E,9R)-4,11, America 11-trimethyl-8-methylidenebicyclo [7.2.0]undec-4-ene)	TCI	C0796
Butyric acid (butanoic acid)	Sigma Aldrich	B103500-100ML
Cyclohexanone	Sigma Aldrich	02482-1ML
Cymene (1-methyl-4-Aldrich propan-2-ylbenzene)	Sigma	C121452-25ML
Decanal	Acros Organics	154971000
Decanoic acid	Sigma Aldrich	C1875-100G
Ethylbenzene	Alfa Aesar	L05908
Eucalyptol (1,3,3-trimethyl-Aesar 2-oxabicyclo[2.2.2]octane)	Alfa	AAA12269AE
Furfural (furan-2-carbaldehyde)	Acros Organics	AC181102500
Geranylacetone (6,10-dimethylundeca-5, 9-dien-2-one)	J&K Scientific	JK520396
Heptanal	Acros Organics	120320500
Heptanoic acid	Acros Organics	164172500
Hexanal	Sigma Aldrich	115606-100mL
Hexanoic acid	Sigma Aldrich	21530-100ML
Indole (1H-Indole)	Sigma Aldrich	I3408-25G
Isobutyric acid (2-methylpropanoic acid)	Alfa Aesar	L04038
Isovaleric acid (3-methylbutanoic acid)	Sigma Aldrich	129542-100ML
Limonene +/- (1-methyl-4-(1-methylethenyl)-cyclohexene)	TCI America	L0046
Linalool (3,7-dimethylocta-1,6-dien-3-ol)	Sigma Aldrich	L2602-100G
Nonanal	Alfa Aesar	A15908
Nonanoic acid	Alfa Aesar	B21568
Octanal	Sigma Aldrich	O5608-100ML
Octanoic acid	Sigma Aldrich	C2875-100ML

REAGENT or RESOURCE	SOURCE	IDENTIFIER
Propanoic acid	Sigma Aldrich	402907-100ML
Styrene	TCI America	S0095
Sulcatone (6-methylhept-5-en-2-one)	Sigma Aldrich	M48805-100ML
Terpineol (2-(4-methylcyclohex-3-en-1-yl)propan-2-ol)	Sigma Aldrich	86480-250ML
Terpinolene (1-methyl-4-propan-2-ylidene-cyclohexene)	Sigma Aldrich	86485-100ML
Valeric acid (Pentanoic acid)	Sigma Aldrich	240370-100ML
Xylene	Acros Organics	422685000
<b>Experimental models: Organisms/strains</b>		
<i>Anopheles gambiae</i> Keele strain	Johns Hopkins Malaria Research Institute	N/A
<i>Anopheles gambiae</i> Kisumu strain	Macha Research Trust, Zambia	N/A
<b>Software and algorithms</b>		
ivTrace	Jens P. Lindemann, Bielefeld University	<a href="https://opensource.cit-ec.de/projects/ivtools">https://opensource.cit-ec.de/projects/ivtools</a>
Matlab R2018b	The MathWorks Inc.	<a href="https://www.mathworks.com/products/matlab.html">https://www.mathworks.com/products/matlab.html</a>
Python 3.8.13	Python Software Foundation	<a href="https://www.python.org/">https://www.python.org/</a>
R	The R Foundation	<a href="https://www.r-project.org/">https://www.r-project.org/</a>
Agilent MassHunter B.07.00,	Agilent Technologies	<a href="https://www.agilent.com/">https://www.agilent.com/</a>
MSConvert v3.0	ProteoWizard	<a href="https://proteowizard.sourceforge.io/">https://proteowizard.sourceforge.io/</a>
MSDIAL v4.90	RIKEN	<a href="http://prime.psc.riken.jp/compms/msdial/main.html">http://prime.psc.riken.jp/compms/msdial/main.html</a>
Metaboanalyst v5.0	Jianguo Xia, McGill University	<a href="https://www.metaboanalyst.ca/">https://www.metaboanalyst.ca/</a>
<b>Other</b>		
Arduino UNO	Arduino	A000066
1/4" vinyl tubing	Cole-Parmer	06405-02
3-way solenoid valve	Clippard	ETO-2-12
Solenoid valve driver	Automate Scientific	ValveLink 8.2
Camera stand with C-mount	Myrin Korea	B00AUJHKC2
Peltier element TEC1-12706	Aideepen	TEC1-12706
Raspberry Pi 3 Model B+	Raspberry Pi	3775
Raspberry Pi Camera Module 2 NoIR	Raspberry Pi	3100
Thermistor WM222C	Sensor Scientific Inc.	WM222C
Aluminum flex ducting, 4" diameter	Lambro	650/AF450UL
Camping Stretches	Teton sports Outfitter XXL camping cot	120A
One-person Swag tent	Kodiak Canvas	8101
Inline Blower 4"	Rule	G4540760
Pulse width modulator	RioRand	RR-6-90V-15A-PSC
Bugdorm-1 Insect Rearing Cage	MegaView Science Co.	DP1000
Round glass bottle	Fishebrand	FB02911944
Night Light	MAZ-TEK YOOUS	MZ3092-4
Digital Illuminance Light Meter	Dr. Meter	LX1330B
IAQ Mini CO2 Meter	CO2Meter	RAD-0302

<b>REAGENT or RESOURCE</b>	<b>SOURCE</b>	<b>IDENTIFIER</b>
Duct to wall connector 4"	Everbilt	596498
Ducting Flange 4"	DL Wholesale	409004
Anemometer	Testo	405i
Mechanical aspirator	John W. Hock Company	Prokopack 1419
IR LED 850nm	Chanzon	100F5T-IR-FS-850NM
3-way duct connector, 4" diameter, Y-shape	MyLifeUNIT	KT18XH072
Pocket Pump	SKC Inc.	220-1000TC
Tenax-TA thermal desorption tubes	Gerstel	020810-005-00
TDU tube storage container	Gerstel	013743-000-00

Author Manuscript

Author Manuscript

Author Manuscript

Author Manuscript